241 (2024) 213159

Contents lists available at ScienceDirect

Geoenergy Science and Engineering

journal homepage: www.sciencedirect.com/journal/geoenergy-science-and-engineering

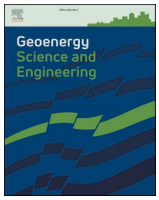

Novel THAI well arrangements for improving heavy oil recovery rate in comparison to that achievable in the conventional THAI in situ combustion technology

Muhammad Rabiu Ado [a], Malcolm Greaves [b], Sean P. Rigby [a,*]

[a] Department of Chemical and Environmental Engineering, University of Nottingham, University Park, Nottingham, NG7 2RD, UK
[b] Department of Chemical Engineering, University of Bath, Claverton Down, Bath, BA2 7AY, UK

ARTICLE INFO

Keywords:
Novel well configurations
Horizontal wells
In situ combustion (ISC)
Enhanced oil recovery (EOR)
Heavy oil/bitumen/tar sand
Reservoir simulation
Toe-to-heel air injection (THAI)

ABSTRACT

The toe-to-heel air injection (THAI) method is an environmentally friendly process for in situ upgrading of heavy oils and bitumen via in situ combustion (ISC). Unlike the conventional ISC that uses a vertical producer, the THAI process uses a horizontal producer (HP) well to produce the upgraded oil to the surface. Recent field data has shown that the THAI process is a relatively low-oil-production-rate technology. These considerations call for innovative solutions so that the oil production rate is improved, whilst propagating a stable, efficient, and safe combustion front. Consequently, this work has provided those solutions. Through numerical reservoir simulations, using CMG STARS, five completely new THAI well configurations, which have been labeled A01, A02, A03, A04, and A05, have been developed and studied, and their performances are compared against that of the conventional THAI process which has wells arranged in a classic SLD pattern (i.e. the best-performing conventional THAI process) and against each other. The THAI arrangements A02-A04, however, assume a horizontal air injection well, which currently is not used in field practice but may be developed in the future. In field practice, THAI is applied in a line drive configuration starting up-dip and going down on the structure whilst taking advantage of the contribution provided by the drainage due to gravity; the expansion is made one way only (by drilling new patterns in one direction only). For this reason, the classic SLD pattern refers to the case where the dip of the reservoir is significant (>2–3°). However, when the dip of the reservoir is not significant ("flat" reservoirs) there is a possibility to expand the process in both opposing directions. This is the case dealt with in this work. All configurations A01-A05 assume expansion of the THAI commercial operation in both directions. Selection criteria have been developed and used to determine the two best performing processes. For example, in terms of long-term stability, safety, and efficiency of the combustion process, a process named model A01 is the best, as it achieved 99.8% oxygen utilisation when compared with any other model. It also achieves oil recovery, due to two years of combustion only, of 30.78% OOIP, which is greater than that in the base case model. Overall, based on the weighted selection criteria, which are developed from the deepest analyses of the quantitative 1-dimensional time-dependent parameters and from thorough analyses of the qualitative 2-dimensional profiles of temperature, the combustion zone in the form of oxygen mole fraction, and the oil-flow dynamics inside the reservoir in the form of oil saturation, then model A01 is the best and is followed by model A03. The overall performance of each of these two novel methods outweighs that of the conventional THAI process. However, model A03 uses a horizontal well for injection, which is not current field practice. Therefore, future developmental work should concentrate on the novel method A01 for upgrading and recovery of heavy oils and bitumen, especially since this is low-carbon, efficient, wastewater-free, and provides upgrading inside the reservoir and hence it has a low surface footprint.

* Corresponding author.
E-mail address: sean.rigby@nottingham.ac.uk (S.P. Rigby).

https://doi.org/10.1016/j.geoen.2024.213159
Received 21 March 2024; Received in revised form 12 June 2024; Accepted 22 July 2024
Available online 23 July 2024

1. Introduction

Approximately, globally, 70% of the total reserves of oil are made up of unconventional oils such as bitumen, heavy oils, tar sand, etc. However, there is no fully-proven, advanced technology that can readily produce these resources efficiently and in an environmentally friendly manner. This is despite the need to develop them for an efficient and smooth transition to carbon-neutral global energy and economic systems. The THAI process is considered one of the technologies that has the green credentials of being a theoretically efficient, low-carbon, and wastewater-free process (Greaves et al., 2008; Rabiu Ado et al., 2017; Turta and Singhal, 2004; Xia et al., 2005). However, this process is yet to be fully understood to the extent that it can have wide acceptance academically and industrially. At the academic level, there are numerous experimental research studies conducted with the aim of advancing the understanding of the THAI process, e.g. see Xia et al. (2002), Xia and Greaves (2002), Zhao et al. (2018), and Zhao et al. (2021). Likewise, there are several lab-scale numerical reservoir simulation studies carried out to enhance our understanding of the THAI and THAI-CAPRI processes, e.g. Greaves et al. (2012c, 2012a), Rabiu Ado et al. (2017, 2018), Ado et al. (2021a, 2021b, 2019), and Ado (2021a, 2021b). Similarly, field-scale reservoir studies conducted with the aim of developing our understanding, and, thereby, providing a systematic process operation design procedure, have been reported, e.g. see Greaves et al. (2012b), and Ado (2020a, 2021c, 2021d, 2021e, 2022a). In addition, there are several older studies that looked at the variation of well configurations to see how these THAI variants compared with the original in terms of key performance parameters, such as oil production rate, ultimately oil recovery, oxygen utilisation efficiency, stability of combustion front, etc. Examples include the study of dry combustion experiments in which a vertical injector (VI) well was used in direct line drive with a horizontal producer (HP) well (VIHP), with 2 parallel HP wells one above the other (VI2HP), and with a single vertical producer (VP) well (VIVP) respectively (Greaves et al., 1993). They found that a higher stability is achieved in the VIHP well configuration, and that higher oil rates are achieved in both the VIHP and the VI2HP configurations when compared to the VIVP pattern. Another study reported on the performance of the VIHP wells pair, horizontal injector (HI) well and parallel HP well (i.e. HIHP) pair, and HIHP well pair at right angles to each other, respectively (Greaves and Al-Shamali, 1996). They found that the HI/VI well placement had a substantial influence on the stability and extent of spread of the combustion front. Furthermore, in all the patterns, ultimate oil recoveries range from 64.3% to 78.8% of oil originally in place (OOIP), depending on whether the combustion is dry or wet (Greaves and Al-Shamali, 1996). An additional experimental study conducted by Xia et al. (2002) found that the HIHP configuration with the wells perpendicular with each other is much more efficient in providing a quick start-up than other well arrangements. Further there is a numerical simulation study conducted by Fatemi et al. (2009) in which they investigated five different wells configurations which are VIHP, VI2HP, HIHP, HI2HP, and 2VIHP wells arrangements respectively. By using various key performance indicators, such as areal and vertical sweep efficiencies, cumulative oil recoveries, CAPEX/OPEX, etc., they found that VIHP and 2VIHP are, respectively, the best and should be used in the field. However, they did not specify the actual location and configuration of the VI wells (i.e. whether staggered or direct line drive (SLD or DLD) is to be used). It is worth pointing out that these are the only studies in the literature that investigated the well configurations for the conventional THAI process and none of them has actually dug deeper to investigate the use of two in-line HP wells in combination with the HI or VI well(s). Also, none of these studies researched the use of two staggered HP wells together with HI or VI well(s).

At the industrial level, Petrobank Ltd. carried out a pilot study of the THAI process in Whitesands, Conklin, Alberta, Canada (Petrobank, 2007, 2008, 2009). The project had 3 VIHP wells pairs with the HP wells having a toe-to-heel length of 500 m and lateral separation of 100 m. Although the project achieved only a partial success in terms of validating the economics of the THAI process and achieving profitably high oil production rates, Petrobank Ltd. deemed it to be a technical success to the extent that they expended and carried out a semi-commercial project in Kerrobert, where another Canadian bitumen reservoir is located. The Kerrobert project had 12 VIHP wells pairs (Turta, 2018) and by the first quarter of 2014, the combined oil production rate was 335 bopd (barrels of oil per day) (Petrobank, 2014). The produced oil had an average API gravity ranging from 13 to 17° API (Turta, 2018). By the third quarter of 2015, the combined oil production rate was 100 bopd (Touchstone, 2015) and by the first quarter of 2016, Touchstone Inc., who had taken over Petrobank Ltd., announced that the Kerrobert THAI project was to be disposed of due to economic losses (Touchstone, 2016). There are three published studies of the lessons learnt and the technical successes of the Kerrobert THAI project (Turta et al., 2020; Wei et al., 2020a, 2020b). In two of these studies (i.e. Wei et al. (2020a, 2020b)), it is found that the relationship between fluids production rates and air injection rate is non-linear and that there is air injection rate limit beyond which no appreciable gain in oil production rate, and thus cumulative oil recovery, will be obtained. They concluded that the THAI process has a higher energy efficiency than SAGD, but is a very low-oil-production-rate technology than the commercially being-used steam-assisted gravity drainage (SAGD) process. Given the findings from field results, combined with the fact that performance improvements have not been achieved since the researches focused on only the well configurations of the conventional THAI process, the need to overcome the inherent low-oil-production-rate nature of the THAI process has never been so urgent. This is especially so since the vast reservoirs of the unconventional oils are desperately needed to be developed to ensure a smooth transition to a carbon-neutral energy and economic systems is provided. We believe there are numerous ways to provide this solution. Among them includes new well reconfigurations, electrically-enhancing the THAI process, shortening the length of the horizontal producer well, etc. Consequently, the main aims of this paper are to detail the findings from new well configurations that have never been investigated before and show that some of these novel methods perform far better than the conventional THAI process. However, it is noted that, in field practice, THAI is applied in a line drive configuration starting up-dip and going down on the structure, and, in this way, taking into account the gravity contribution advantage; the expansion is made one way only (by drilling new patterns in one direction only). For this reason, the classic SLD pattern refers to the case where the dip of the reservoir is significant (>2–3°). However, when the dip of the reservoir is not significant ("flat" reservoirs) there is a possibility to expand the process in both opposing directions. This is the case we are dealing with in this work. All configurations A01-A05 assume expansion of the THAI commercial operation in both directions. Furthermore, it should be noted that the classic THAI-SLD process referred in this work is studied in the so-called flat formation (i.e. the model reservoir onto which the classic THAI-SLD process was run has relatively very low dip (<2–3°)). This is justified given that the properties of all the model reservoirs in this work are those of the typical Canadian Athabasca bitumen reservoir, which in reality has a relatively very low dip. Additionally, it should be noted that, in three (3) of the novel THAI configurations studied and detailed in this paper, horizontal injectors are used. However, since horizontal injectors are not used in field practice, it is anticipated that the results from their simulation may be used in the future, when technological advances and economic calculations will justify that use.

2. Construction of reservoir models having novel wells configurations

Since it is found from the Canadian Kerrobert project, which was executed by Petrobank Ltd. between 2011 and 2016 (Petrobank, 2013, 2014; Touchstone, 2015, 2016), that the conventional THAI process is a low-oil-production-rate technology (Turta et al., 2020; Wei et al., 2020a,

2020b), the need to improve oil production rates and recovery factors is not only efficient and profitable but also it will allow earlier realisation of returns of investment, thereby reducing the risks from the oil market volatilities. Therefore, novel well configurations, which have never been developed before, are shown, researched, and discussed in this work and, after simulating them using the CMG STARS reservoir simulator, their respective performance in terms of oil production rate, cumulative oil recovery, oxygen production, oil saturation distribution profile, temperature distribution profile, and shape and stability of combustion zone are compared against that of the conventional THAI process. Prior to specifying input parameters, the reservoir domains with these new well configurations and their dimensions are presented first. They are subsequently followed by the common input parameters that are required for simulating any in-situ-combustion-type process.

2.1. Reservoir dimensions and new well configurations

All the models are constructed using the Computer Modelling Group's (CMG's) model Builder which works in conjunction with the CMG's reservoir simulator, STARS. All the models have the same reservoir volume and the same corresponding surface areas in each of their 6 faces. All in all, the models are correspondingly of the same size.

2.1.1. Base case reservoir with SLD wells configuration

The conventional THAI process has been piloted and operated at semi- and full commercial scales with the vertical injector (VI) and horizontal producer (HP) wells configured in a direct line drive (DLD) pattern (Petrobank, 2008; Turta, 2018). This is one of the two possible configurations that have been identified by Turta (2018). The other pattern is the use of two VI wells arranged in a staggered line drive (SLD) configuration with the HP well, which has been field-tested in India only (Turta, 2018). This latter one is found to be more efficient, stable, and easier to operate by recently published studies which were conducted by Ado (2021a, 2021d). Consequently, the wells in the base case of the conventional THAI process in this study are arranged in a SLD pattern, as can be seen in Fig. 1. This base case model is referred to as THAI-SLD.

2.1.2. Model A01: well orientations and reservoir dimensions

This reservoir numerical model consists of two in-line horizontal producers (P2A and P2B) with two vertical injectors arranged in a staggered line drive configuration as depicted in Fig. 2. The injectors are located at the top of the reservoirs, each at horizontal offset distance of 7 m away from the toe of each horizontal producer, namely P2A and P2B respectively. The main differences between this model A01 and the base case THAI-SLD model are the relocation of the VI wells to the centre of the reservoir along the axial direction of the HP wells, the splitting of the horizontal producer into two, and the relocation of the toes of the HP wells to the centre of the reservoir (Fig. 2). This new well configuration has been considered because it was found, in a recently published study (Ado, 2021e), that most of the oil enters into the HP well via the toe and, in the absence of impermeable wall behind the toe, the mobilised upgraded oil will be lost. Consequently, the oil that would have been lost is now forced to enter into either of the toe HP wells and thus causing increase in oil recovery factor.

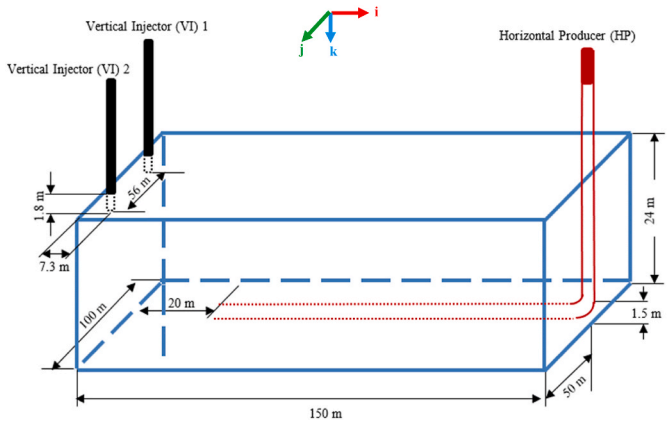

Fig. 1. Reservoir domain and dimensions, and the wells arranged in a staggered line drive (SLD) configuration for the base case conventional THAI process. This is a model reservoir with a relatively very low dip (i.e. is a model of a flat formation).

2.1.3. Model A02: well orientations and reservoir dimensions

This reservoir numerical model is similar to model A01 except that one short horizontal injector (HI) well was used, as opposed to the two vertical injectors used in model A01. The HI well was placed 17 m vertically above the horizontal producers. All the wells are located on the vertical mid-plane of the reservoir thereby making them to be in a direct line drive (DLD) configuration. From the toe to the location that is 8 m along each of the HP well, each HP well is directly under the HI well, as can be seen in Fig. 3. This novel well arrangement is designed with the aim of establishing a well-distributed and structured combustion front that rapidly covers a larger volume of the reservoir so that excellent heat distribution can be achieved which, in turn, will accelerate oil production rate. However, this model will be easily prone to early oxygen production and hence breakthrough.

2.1.4. Model A03: well orientations and reservoir dimensions

In the reservoir numerical model A03, the HP wells arrangement and the length of the HI well are, respectively, similar to those in model A02. However, in model A03, the HI well is oriented perpendicularly to the axial direction of the HP wells, as depicted in Fig. 4. This configuration is designed with the aim of achieving a widely well-distributed and stable combustion zone whilst providing high oil recovery rates. Unlike in model A02, this model will be less likely to have early oxygen production and thus breakthrough.

2.1.5. Model A04: well orientations and reservoir dimensions

This reservoir numerical model has a HI well dimension and orientation that is similar to that in model A03. The horizontal producer (HP) wells, however, are no longer along the same vertical mid-plane. Rather, the HP well P2A is placed 22 m to the right of the vertical mid-plane, while the HP P2B is placed 22 m to the left of the vertical mid-plane. These modifications mean that the two producers are separated by a lateral distance of 44 m in the ***j*** direction, as shown in Fig. 5. By relocating the HP wells to either side of the reservoir, it is thought that the oil mobilisation rate will substantially improve. This is because the mobilised upgraded oil that would have otherwise accumulated at the base of the reservoir, and in the adjacent vertical ***i-k*** planes, will be easily captured by the two wells and hence gets produced to the surface. Furthermore, this novel well arrangement is developed with the goal of also achieving a widely well-developed and stable combustion front, while at the same time enhancing oil production rates and recovery factors.

2.1.6. Model A05: well orientations and reservoir dimensions

This new reservoir numerical model A05 is very similar to model A02 except that a single vertical injector (VI) well in a direct line drive (DLD) arrangement with the two HP wells is used in the former. (see Fig. 6). Model A05 is designed with the aim of increasing oil production rates and recovery factors especially since a recently published study by Ado (2021e) has shown that unless there is an impermeable wall behind the toe of the HP well in the conventional THAI process, mobilised upgraded oil will be lost due to backward drainage.

2.2. Reservoir domain and equation discretisation

After developing the reservoir dimensions and the well

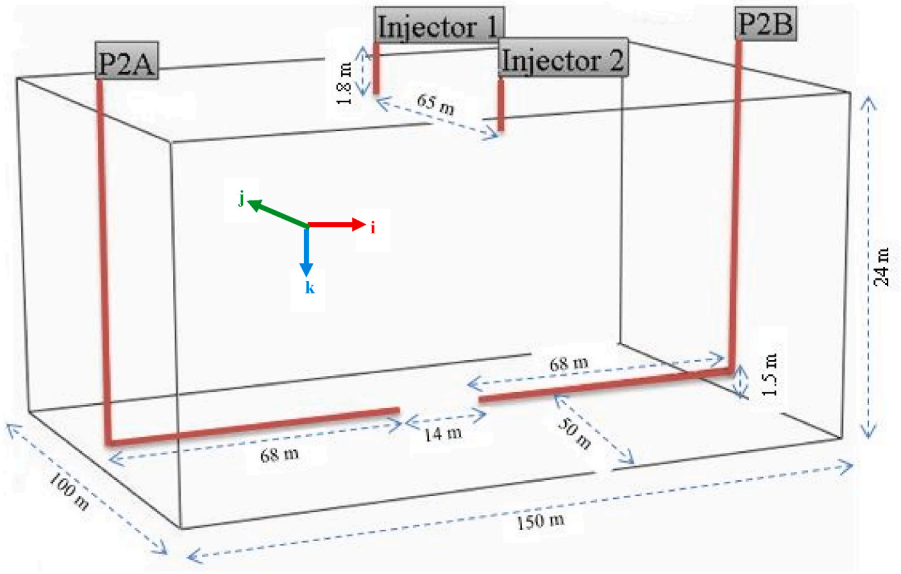

Fig. 2. Reservoir domain and dimensions, and the wells arranged in an SLD configuration for model A01 in which two HP wells, which are located on the same vertical mid-plane, are used together with the two VI wells. This configuration has the flexibility of being possibly expanded in opposing directions for a commercial operation for flat formations.

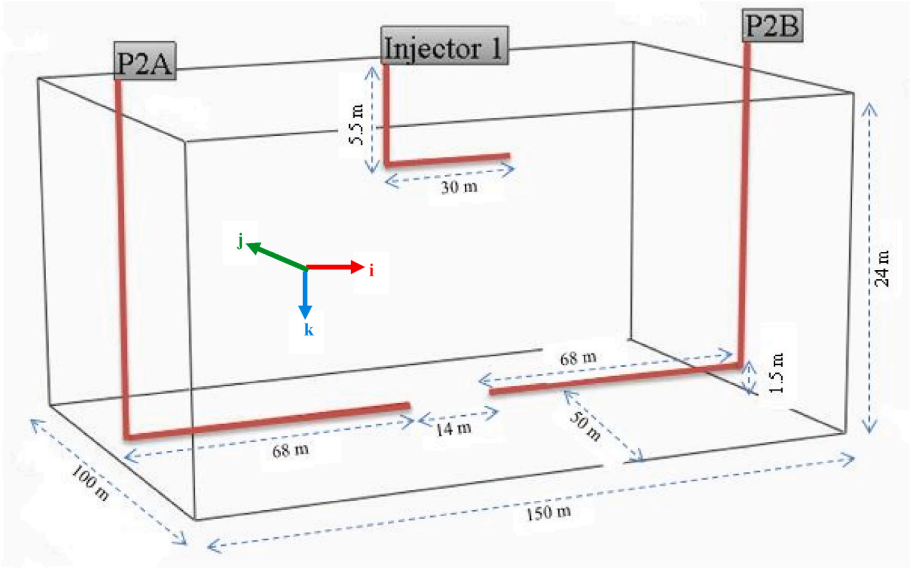

Fig. 3. Reservoir domain and dimensions, and the wells arranged in a DLD configuration for model A02 in which two HP wells, which are located on the same vertical mid-plane, are used together with the HI well whose horizontal section points in the ***i*** direction in a toe-to-heel manner. This configuration has the flexibility of being possibly expanded in opposing directions for a commercial operation for flat formations.

configurations, the next task is to divide the reservoir domain, that is to be numerically simulated, into a number of grid blocks. In each of the models, the reservoir is divided into 30 grid points in the ***i*** direction, by 19 grid points in the ***j*** direction, by 7 grid points in the ***k*** direction, thereby generating 30 × 19 × 7 parent grid blocks. To capture the full physics of the combustion front, along the ***i*** direction, each parent grid block is divided or refined into 3 child grid blocks. Similarly, for the same purpose, along the ***j*** direction, each parent grid block is divided or refined into 3 child grid blocks. Thus, the total number of grid blocks is 90 × 57 × 7. Then, the highly non-linear partial differential equations governing the physicochemical transport processes that take place in the in-situ-combustion-type processes, and which have been discretised and thus converted to algebraic equations, are solved for each grid block using a fully implicit finite difference method in the CMG STARS software. However, prior to that, in order to accurately account for the transport processes inside the horizontal producer well(s) in each model, STARS allows the use of a discretised wellbore model entitled ''WELLBORE''. Therefore, STARS automatically divides the HP well domain into a number of grid blocks, and thus the overall number of grid blocks (i.e. those of the reservoir model and those of the wellbore model) becomes 38,500, which is in accordance with the other published studies (Ado, 2020a, 2020b, 2020c, 2020d, 2020e). That, hence, allows the algebraic equations resulting from the discretised reservoir model, and those from the discretised wellbore model, to be solved simultaneously in STARS using a parallel processing solver. Therefore, these same procedures are implemented in each model. However, to run the numerical simulations, the properties of the fluids and the solids in the reservoir must first be identified and specified. Similarly, the reactions

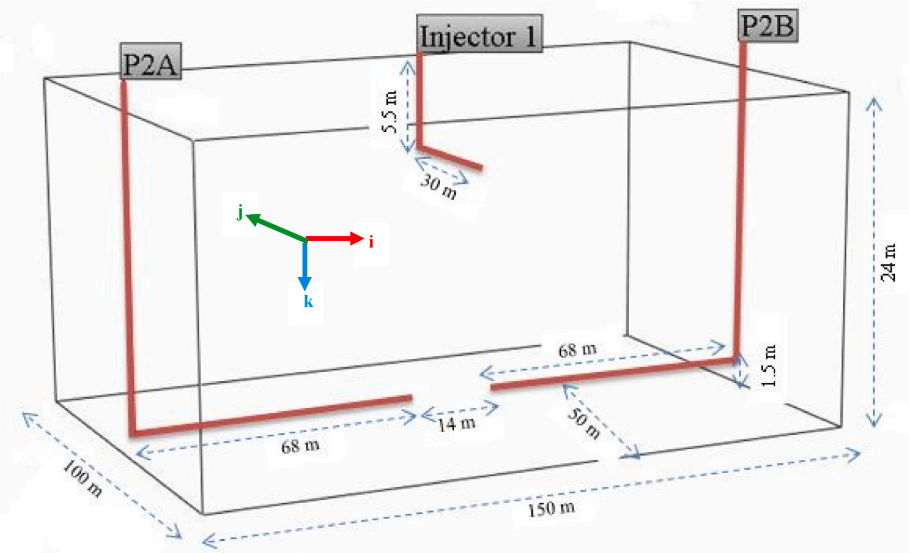

Fig. 4. Reservoir domain and dimensions, and the wells arranged in an SLD configuration for model A03 in which two HP wells, which are located on the same vertical mid-plane, are used together with the HI well whose horizontal section points in the ***j*** direction in a toe-to-heel manner. This configuration has the flexibility of being possibly expanded in opposing directions for a commercial operation for flat formations.

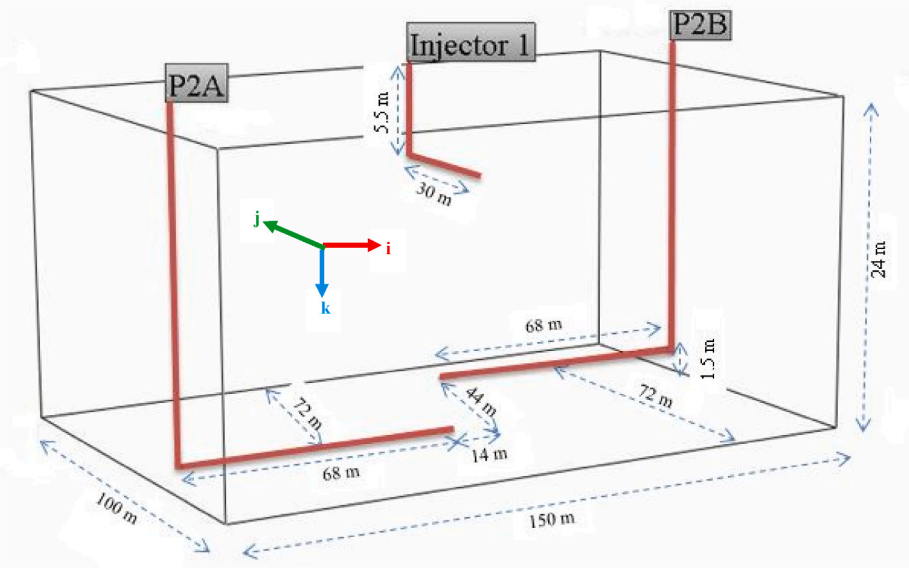

Fig. 5. Reservoir domain and dimensions, and the wells arranged in an SLD configuration for model A04 in which two HP wells, which are located on the vertical planes that are adjacent to the vertical mid-plane, are used together with the HI whose horizontal section points in the ***j*** direction in a toe-to-heel manner. This configuration has the flexibility of being possibly expanded in opposing directions for a commercial operation for flat formations.

schemes and their kinetics parameters must be specified, as can be seen next. Prior to this, however, we would like to state that we had conducted grid sensitivity studies for the laboratory-scale validated model from which these models are derived, and we found that the results converged onto each other. Additionally, we would like to state categorically that all the simulation results are considered acceptable only when the final material balance error fell within the 0.01%–1% acceptable level as is specified in the CMG STARS user manual. Thence, we monitored the material balance error as the simulation of each model was run and made sure we only accepted the results when it satisfied the set criterion, which was the same for all the models. It can, therefore, be concluded that there is no numerical error that was capable of causing the asymmetries observed in some of the models, as will be seen subsequently.

2.3. Reservoir input parameters

Prior to numerically simulating any in-situ-combustion-type process, quite a large number of input variables are required especially since the physicochemical processes are highly complex. This is not only because of the complexity associated with the large number of hydrocarbon components which must be represented by pseudo-components but also due to the multiphase reactive transport systems in porous medium nature of the processes. As a result, the input parameters used in this work are summarily discussed as can be seen next. However, before that, it is worth noting that the oil mimicked in this work is that of the Canadian Athabasca bitumen reservoir and therefore, its properties, which have been reported in previous work (Ado et al., 2019; Rabiu Ado et al., 2017, 2018), are also used throughout this work. It should be noted that all of the aforementioned models have the same input parameters. They

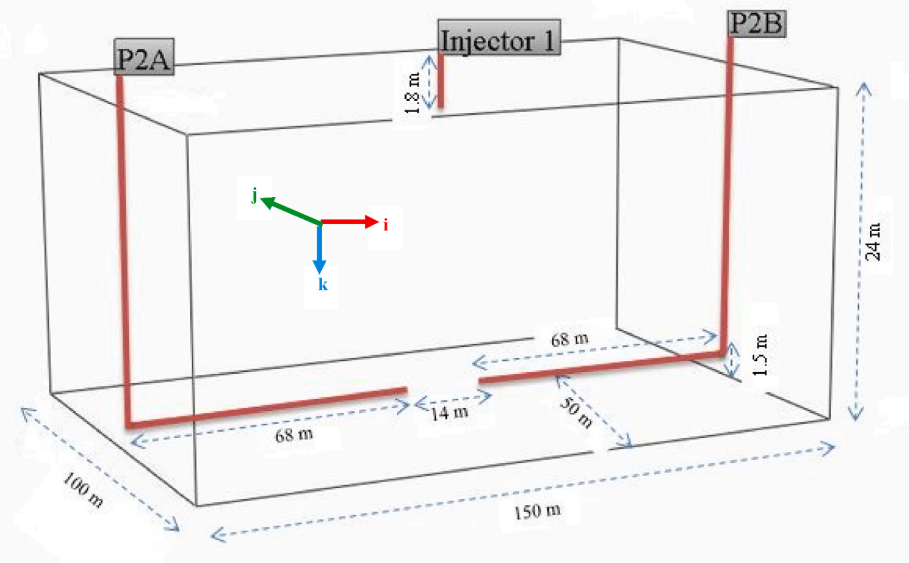

Fig. 6. Reservoir domain and dimensions, and the wells arranged in a DLD configuration for model A05 in which two HP wells, which are located on the same vertical mid-plane, are used together with a VI well. This configuration has the flexibility of being possibly expanded in opposing directions for a commercial operation for flat formations.

only differ in terms of the well configurations.

2.3.1. *Reservoir petro-physical and initial condition parameters*

The Athabasca bitumen reservoir petro-physical and initial condition parameters, namely the vertical and horizontal absolute permeabilities, porosity, initial saturations of oil, gas, and water, and the initial pressure and temperature, as used throughout this work, can be found in Table 1. More details concerning them can be found elsewhere (Rabiu Ado, 2017). The relative permeability curves for the oil/water and gas/oil as used throughout this work can be found in Rabiu Ado (2017) and, as a consequence, they are not reproduced here in order to conserve space.

2.3.2. *Reservoir rock and fluid properties*

The thermal and non-thermal properties of the Athabasca bitumen reservoir rock and the reservoir fluids as used throughout this work have been taken from Ado (2022b) and to save space, they are not reproduced here.

2.3.3. *PρT properties, viscosity, and K-values of the Athabasca bitumen*

Firstly, the density of the Athabasca bitumen at a temperature of 20 °C, as used in this work, is 1011 kg/m^3 (i.e. it is at a quality of 8.46° API gravity) and its initial viscosity at a temperature of 20 °C, as used in this work, is 1.8086×10^5 cP. However, due to the very large number of compounds that make up bitumen, it is impossible to represent the whole mixture using the individual hydrocarbon components that it is made up of. Moreover, it is impractical to use a very large number of components when simulating the in-situ-combustion-type processes. Thus, a small number of oil pseudo-components, which are, themselves, made up of a number of hydrocarbon compounds that belong to a specified range of boiling temperatures, are used to represent the bitumen mixture. Therefore the pressure, density, and temperature (PρT) properties of each of the three oil pseudo-components making up the bitumen have been detailed in the validated models developed and reported by Rabiu Ado (2017) and Rabiu Ado et al. (2018, 2017), and are reproduced in this paper for ease of reference, as can be seen in Table 2. Likewise, the composition, in mole percent, of each oil pseudo-component (i.e. the split) can be found in Table 2. However, the viscosity of each oil pseudo-component, as function of temperature, and their respective vapor-liquid equilibrium (VLE) K-values, as a function of both temperature and pressure as calculated from the data in Table 2 using the Wilson's equation (Almehaideb et al., 2003), are detailed in Rabiu Ado (2017) and for this reason, they need not be presented in this article as the reader can refer to the provided reference.

Table 1
Reservoir petro-physical and initial condition parameters.

Reservoir petro-physical and initial condition parameters	Field-scale values
Porosity	34%
Horizontal absolute permeability, k_h (mD)	6400
Vertical absolute permeability ratio, k_v (mD)	3450
Reservoir initial water saturation, S_w	20%
Reservoir initial oil saturation, S_o	80%
Reservoir initial gas saturation, S_g	0%
Reservoir initial temperature (°C)	20
Reservoir initial pressure (kPa)	2800

2.3.4. *Kinetics scheme and its parameters*

Experiments (Greaves et al., 2008; Xia et al., 2005), simulations (Greaves et al., 2012c; Rabiu Ado et al., 2017), and field findings (Turta et al., 2020; Wei et al., 2020a, 2020b) have shown that the thermal cracking and coke combustion reactions are the dominant reactions in the THAI process as applied to Canadian Athabasca bitumen. As a result, the THAI process operates in a high-temperature-oxidation (HTO) mode in which the combustion front has high temperatures. To simulate the THAI process, the aforementioned reactions, and the combustion reactions of the individual oil pseudo-components which are found to have negligible effects, are required and thus must be inputted together with their Arrhenius kinetics parameters. However, as shown by many researchers, the lab-scale validated Arrhenius kinetics parameters cannot be used to simulate a field-size reservoir. This is because of the differences in the length- and time-scales. For these reasons, systematically up-scaled and well-tested field-scale Arrhenius kinetics parameters, which can be found in Ado (2020b), are used in this work. It should be noted that the lab-scale kinetics scheme and the respective activation energy of each reaction are the same as those in the field-scale as these are independent of scale (Rabiu Ado et al., 2017). Since all of the reaction schemes and their kinetics parameters are reported in detail in Rabiu Ado et al. (2017) and Ado (2020b), and in order to conserve space, the reader is referred to these references for further information.

Table 2
Bitumen pseudo-components and their composition, molecular weight, boiling temperature, PρT properties, and eccentricity.

Oil pseudo-component	Composition (mol %)	Molecular weight (kg/kmol)	Boiling temperature T_B (°C)	Critical pressure P_c (kPa)	Density ρ (kg/m^3)	Critical temperature T_c (°C)	Acentric factor ω
LC	42.50	210.82	281.47	1682.88	828.24	464.68	0.62
MC	23.91	496.81	549.67	1038.46	961.66	698.53	1.18
IC	33.59	1017.01	785.78	729.22	1088.04	940.36	1.44

2.3.5. Boundary conditions

Throughout each reservoir model, a no flow boundary condition is applied except through the wells that have fluids being injected and produced. Via the vertical injector (VI) well(s), saturated steam at a pressure of 5500 kPa, and having a quality of 0.8, is injected for the purpose of pre-ignition heating at the combined maximum possible total rate of 495 bbl day^{-1} cold water equivalent (CWE) for a period of 104 days. This implies that the maximum cumulative steam injected in any of these models is 8185 m^3 CWE, which is roughly the same as the maximum that was cumulatively injected in the Athabasca THAI application conducted by Petrobank Ltd. Although, it may be lower than this depending on the maximum bottom hole pressure around the outlet of the injection well(s). Thereafter, air is injected at the rate of 20,000 Sm^3/day for a period of two years. In the case of the horizontal producer (HP) well(s), each HP well is assigned a minimum bottom hole pressure (BHP) of 2800 kPa and a maximum liquid production rate of 60 Sm^3 h^{-1} which is based on the up-scaled production rate. The STARS simulator automatically determines which of the boundary conditions to use depending on which targeted one is violated. With regard to the heat loss, it is assigned that heat is lost via the overburden and underburden only. Since fluids do not cross the boundary except via the wells, it implies that the heat loss via the overburden and underburden takes place due to conduction only, which is accounted for by specifying the heat capacity and thermal conductivity of the rocks overlying and underlying the bitumen reservoir. It should be noted that these parameters are not specified here. Rather, they can be found in the thesis of Rabiu Ado (2017) which this work builds upon.

2.3.6. Limitations of the simulation

All the model reservoirs considered in this work have ideal geological features, such as being homogenous, containing no bottom water, having no gas cap, and having extremely low to no inclination. Furthermore, in the novel THAI arrangements A01 to A05, the HP wells can be considered short since each of them has a horizontal-section length of half that of the HP well of the base-case model. Therefore, the simulations of A01 to A05 involve studying processes with short wells, thereby implying that the effects of the length of the horizontal section of the HP wells are not investigated. Additionally, all the models have been simulated for a process operating period of at most 834 days and hence the full effects of full length of the horizontal section of the HP wells have not been investigated yet. That means, the process operating duration for each model is not long enough to allow for that, which by implication means that only the segment of the HP well close to the toe region in each model is investigated. This is caused by the fact that, with the extension in process time, the simulation run-time gets extremely expensive as the time steps get impractically small. It is important to also note that, given the preceding limitation which is imposed by the simulator, the combustion front in some models (i.e. in models A01 and A02) did not fully reach, and thus is not fully anchored to, the toe of the horizontal producer(s). However, if the infinitesimal changes in time steps issues can be overcome, then the process operating time can be extended to obtain better understanding of the combustion front and oil flow dynamics inside the reservoir and around the heel region of the HP wells. Moreover, it is worth highlighting, at this stage, that the percentage of oxygen in the produced gas stream is found to be generally higher in these models compared to that in the current THAI application in the field.

3. Results and discussion

The key performance parameters that are used to assess the success or otherwise of the in-situ-combustion-type processes are shown, compared, and discussed as follows. This allows determination of the models for which their well configurations provide the best performance in terms of oil production rate, cumulative oil recovery, structure and stability of the combustion zone in form of oxygen distribution, reservoir dynamics in form of oil saturation distribution, and temperature distribution.

3.1. Oil production rates, and cumulative oil production and recoveries

In each model, steam is injected at the combined rate of 495 bbl day^{-1} cold water equivalent (CWE) for 104 days prior to the commencement of air injection. Within that period, oil production began at the earliest in model A05, which was then followed by model A02, which, in turn, was followed by model A04, which then was followed by model A03, and, then the base case model (THAI-SLD) (Fig. 7). The model that had the longest delay in oil production was A01. This means that the longest time, of around 8 weeks, before fluid communication was established between the wells in model A01 is unlike that in model A05 in which communication was established in less than two weeks (Fig. 7). The reason for the earliest start of the oil production in model A05 is due to the fact that the 2 HP wells and the VI well are on the same vertical mid-plane (i.e. they are in direct line drive configuration) and. therefore, the steam did not have to travel as far before it reached the toes of the 2 HP wells. On the other hand, the reason for the longest delay in model A01 is due to the very long lateral distance separating the toes of the 2 HP wells from the shoes of the 2 VI wells which are located on planes that are adjacent to the vertical mid-plane where the 2 HP wells are. In models A02, A04, A03, and the base case, the fluid communication between the wells is established in 4, 5, 6,

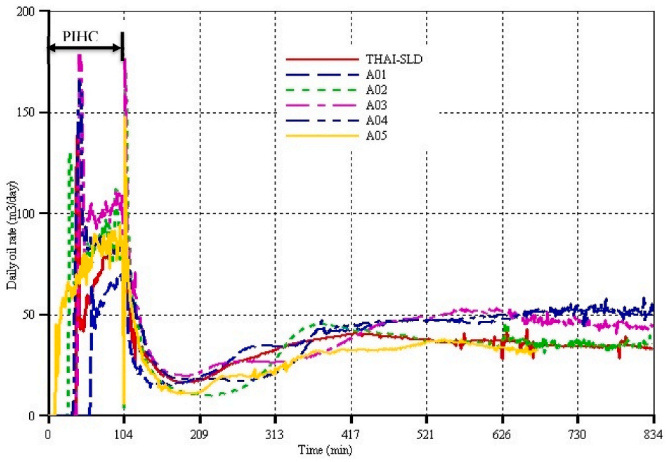

Fig. 7. Combined oil production rates as function of time. Note that the THAI-SLD model has a single HP well which is unlike the other models that each has two HP wells.

and 6 weeks respectively (Fig. 7). Thus, a general pattern can be seen, in which the closer the shoe(s) of the VI well(s) or the horizontal section of the HI wells to the toes of the HP wells, then the earlier the start of the oil production. Hence, a question might be asked about why, despite the fact that 2 VI wells in staggered line drive configuration are used in the base case THAI-SLD model, the oil production started much earlier than in model A01. The answer is due to the fact that the 2 VI wells in THAI-SLD model are closer to the reservoir boundary (i.e. they are located in the first ***j-k*** plane on the left side of the reservoir) and hence steam had a smaller horizontal area to spread within thereby forcing it to advance faster in the downward direction. This resulted in the forcing of the mobilised oil to reach the toe of the HP well and get produced quickly. Generally, all the models have similar trends of oil production rate curves (Fig. 7) in which there are instantaneous peaking of the oil rates at the start of production. Then there are sudden drops in the oil rates before they, thereafter, steadied out at oil rate values of between roughly 50 m^3/day and 100 m^3/day up to the time when air injection just began. Throughout most of the pre-ignition heating cycle (PIHC) period, the oil production rate in model A03 lies above those of the other models. It is followed by model A02, then A04, A05, THAI-SLD, and A01 in this order. However, due to the earlier-identified variabilities in the time at which the oil production began in the models, by the end of the 104 days of the PIHC, the combined cumulative oil recoveries in models A02, A03, and A05 respectively are approximately the same and are higher than that of model A04 (Fig. 10). That of the base case model THAI-SLD is lower than that of the model A04 but substantially higher than that of model A01 as will be discussed later (Fig. 10).

In each model, the combined air injection rate is 20,000 Sm^3/day, except for model A01, where two VI wells are used, the air injection rate via each of the two VI wells is 10,000 Sm^3/day. All the models behaved in an exactly similar manner when air injection began and when ignition was achieved just after 104 days of the steam injection period. The sudden peaking in oil production rate in each model is caused by an 'air-pushing effect' on the oil, or air transferring its momentum to the already steam-mobilised oil in the vicinity of the injector well(s) and toe of the HP well(s) of each model. Once all of the steam-mobilised oil is fully displaced, there is a rapid drop and subsequently gradual decline of the oil production rate in each model (Fig. 7) until they reached minimum rates at around 174 days for all models (i.e. 10 weeks after the start of air injection) except model A02 which reached the minimum at around 220 days (i.e. around 17 weeks after the start of air injection). All the models stayed at those minimum oil rates until around 209 days except model A02 which stayed at the minimum a little longer, until 244 days. These occurrences are caused by an air-cooling effect in which there is competition in heat utilisation between the injected air and the cold oil zone downstream of the combustion front. The oil rates stayed at the minimum when the rate of heat utilisation by the injected air and by the cold oil layer and reservoir rock that are downstream of the combustion zone become equal to the rate of heat generation and release by the coke combustion reaction. When the rate of heat generation and release became larger than that needed by the air and the cold oil layer and reservoir rock ahead of the combustion zone, then oil mobilisation and production in each model started to gradually increase until it reached peaks at 365 days in model A02, at 417 days in THAI-SLD model, at 540 days in model A05, 570 days in model A03, and 670 days in models A01 and A04 respectively. Beyond these times, there were slow declines but subsequent steadying-outs of the oil rates in models A02, A03, A05, and the base case THAI-SLD, respectively, until the end of the 2 years of the combustion period, and there were steadying-outs at more or less the same production rates of approximately 55 m^3/day in models A01 and A04, respectively. However, there were variations in the increasing, steadying out, and decreasing trends of the oil production rates and, to provide details as to why each model behaves the way it does, the combined oil production rate, cumulative oil recovery, and cumulative oil production per well of each model are discussed on a model-by-model basis.

3.1.1. Model A01: oil production and recovery

Recall that this model uses two vertical injector (VI) wells arranged in a staggered line drive configuration with the two horizontal producer (HP) wells (i.e. P2A & P2B). During the pre-ignition heating cycle (PIHC) in model A01, oil was preferentially displaced towards the HP well P2A which is as a result of the overlapping of the expanding high oil saturation rings originating from the shoe of each VI well. The rings are formed due to heat and momentum transferred from the injected steam. As steam was continuously injected through both injectors, the edges of the rings were displaced to the extent that they can no longer expand laterally (i.e. the two chambers/rings have merged and become a single chamber (for an example, see Fig. 15a and b)) and their common intersection near the centre of the reservoir disappeared. Further steam injection after this point resulted in propagation of axial and top-down steam fronts. As the steam fronts push further down, the mobile oil high saturation zone first reached the toe of HP well P2A and thus created a communication pathway between the injectors and P2A producer. These are what caused the longest delay in the start of oil production in this model (Fig. 7) and what provided the preferential channel through which most of the earlier mobilised oil flowed and got produced to the surface via HP well P2A.

At the end of 104 days of PIHC, 2.85% of the oil originally in place (OOIP) is recovered which is mainly via producer P2A (Figs. 8 and 9). It should be recalled that 10,000 Sm^3/day of air is injected via each injector and this is maintained constant throughout the 2 years' combustion period. Once air injection is started, the combined oil production rate declines gradually to a lowest value of 15 m^3/day before increasing steadily and stabilising at around 46 m^3/day after 270 days of combustion (Fig. 7). As the combustion front continued to expand and heat is further distributed into the reservoir, more mobilised oil is displaced towards the toe of producer P2B which made it come on stream after 520 days of combustion. This resulted in a further steady increase in combined oil production rate (Figs. 7–9). The slow increase is sustained up to the end of the 2 years of the combustion period, while the oil rate stabilises at around 55 m^3/day. Fig. 10 shows the combined cumulative oil recovery due to both PIHC and combustion. For model A01, around 33.63% OOIP is recovered after roughly 28 months of operation (i.e. of steam injection, air injection and combustion, and production). Around 95% of the combined cumulative oil recovery is produced via HP well P2A thereby showing that the HP well P2B is redundant in this model. However, Fig. 9 shows that the increase in cumulative oil production via HP well P2B is likely to be sustained for a very long time. For the two years of combustion only, Fig. 11 shows that the combined oil recovery is 30.78% OOIP which is higher than that achieved in the base case model by a margin of 4.28% OOIP. Since the combustion front did not reach the toe of either of the producers, it is likely that more oil will be recovered whilst the process operates stably and efficiently.

3.1.2. Model A02: oil production and recovery

Recollect that model A02 is similar to A01 in terms of the use of two in-line HP wells but is different due to A02 having a single horizontal injector (HI) which has a short horizontal-section length of 30 m. As all the wells were directly on the same vertical mid-plane (i.e. in a direct line drive (DLD)), communication between the wells is easily established once steam injection was started. Oil displacement due to steam condensation is found to be symmetrical as the injector directly overlies the two producers. By the end of 104 days of PIHC, 6.81% of OOIP (oil originally in place) was recovered through both producers with each producer accounting for approximately 50% of the recovered oil (Figs. 7–9). As the air injection is started, the combined oil production rate declined steadily before reaching a lowest value of around 10 m^3/day at roughly 220 days. As the combustion front expanded and heat is distributed into the reservoir, more oil is mobilised, which resulted in a gradual increase in oil production rate before reaching a maximum value of 46 m^3/day at around 270 days after the start of air injection (Fig. 7). The combined oil production rate then decreased before it

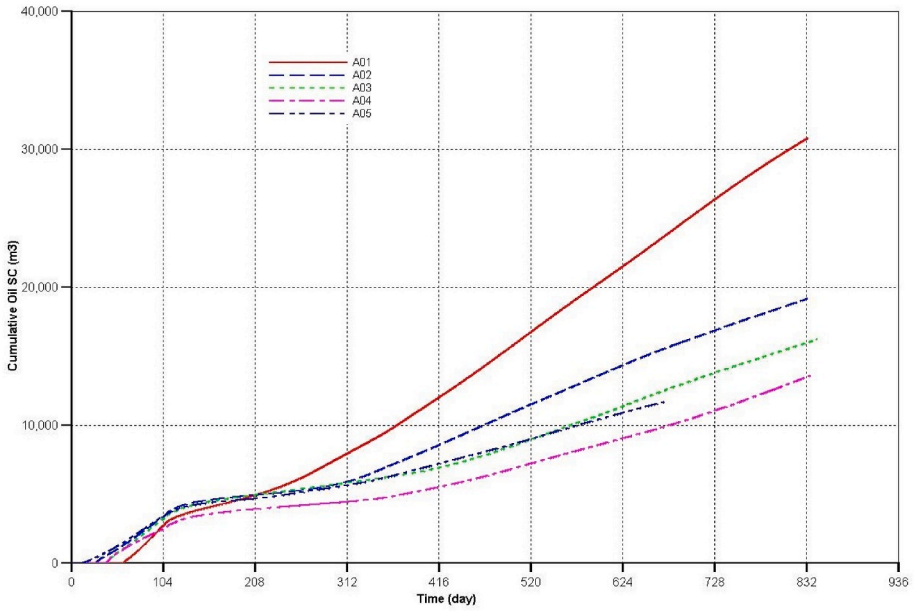

Fig. 8. Cumulative oil production from HP well P2A as function of time. Note that the THAI-SLD model has a single HP well and thus is not included here.

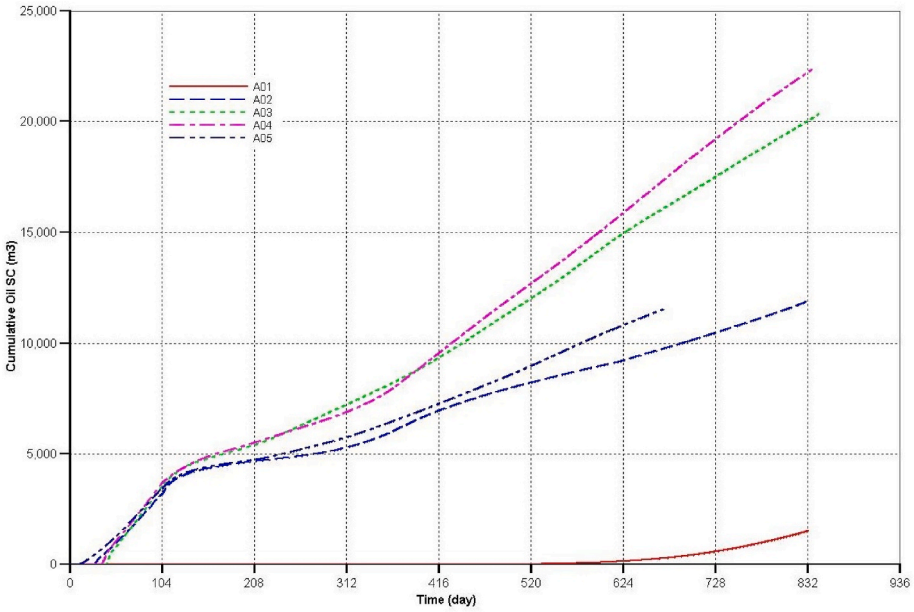

Fig. 9. Cumulative oil production from HP well P2B as function of time. Note that the THAI-SLD model has a single HP well and thus is not included here.

stabilised at 36 m^3/day at 520 days up to the end of the two years of combustion period. After 104 days of PIHC and two years of combustion, around 19190 m^3 and 11910 m^3 of oil were recovered from HP wells P2A and P2B respectively (Figs. 8 and 9). These mean a combined cumulative recovery of 32.31% OOIP (Fig. 10). It then follows that producer P2A accounted for approximately 62% of the combined cumulative oil production. The cumulative percent recovery due to the two years of combustion only is 25.5% OOIP (Fig. 11). In comparison to model A01, this model A02 has a lower oil recovery by a margin of 5.28% OOIP during the combustion period only. Furthermore, the recovery in this model is lower than in the base case model by a margin of 1.00% OOIP (Fig. 11). In this DLD arrangement, it is found that the combustion front reached the two of the HP wells quite rapidly thereby implying that prolonging the operation time will be unsafe and inefficient and hence uneconomical.

3.1.3. *Model A03: oil production and recovery*

In this model A03, just like in the previous models A01 and A02, the HP wells are in-line with each other, located in the vertical mid-plane. However, the horizontal injector (HI) well which has a short horizontal-section length of 30 m is located at right angles to the axial direction of the HP wells, thus making the arrangement to be in a staggered line drive (SLD) pattern. In this model, the oil displacement due to the PIHC is symmetrical around the two producers. This is due to the fact that the HI well has perforation that lies on the same plane as the HP wells and, as a result, the high oil saturation zone was displaced toward both producers. By the end of 104 days of PIHC, 6.98% OOIP was recovered with both producers contributing around 50% of the recovered oil just like in model A02 (Figs. 7–9). Just like in the previous two models (i.e. A01 and A02), the combined oil production rate dropped steadily to a lowest value of 20 m^3/day at around 70 days after the start

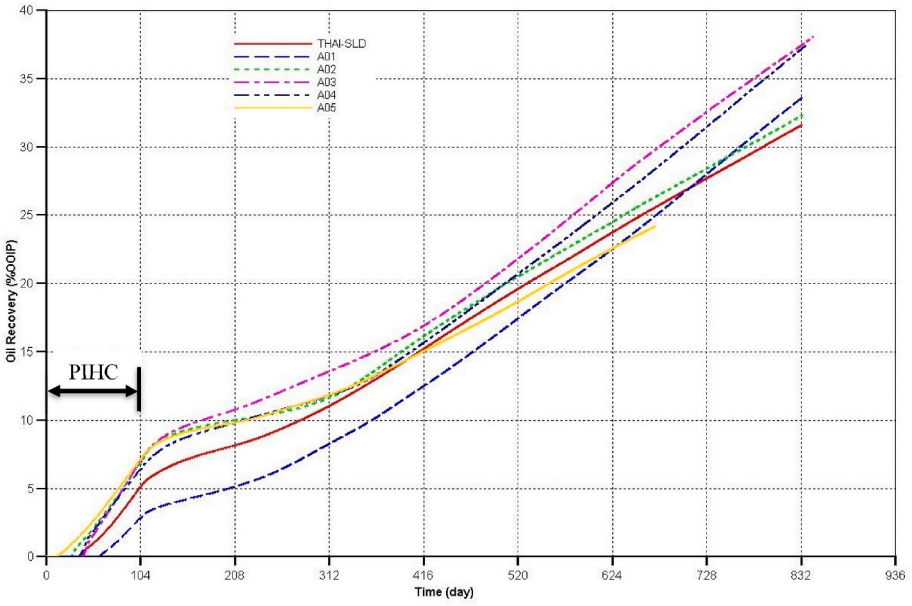

Fig. 10. Combined cumulative oil recoveries due to steaming and combustion as function of time. Note that the THAI-SLD model has a single HP well which is unlike the other models that each has two HP wells.

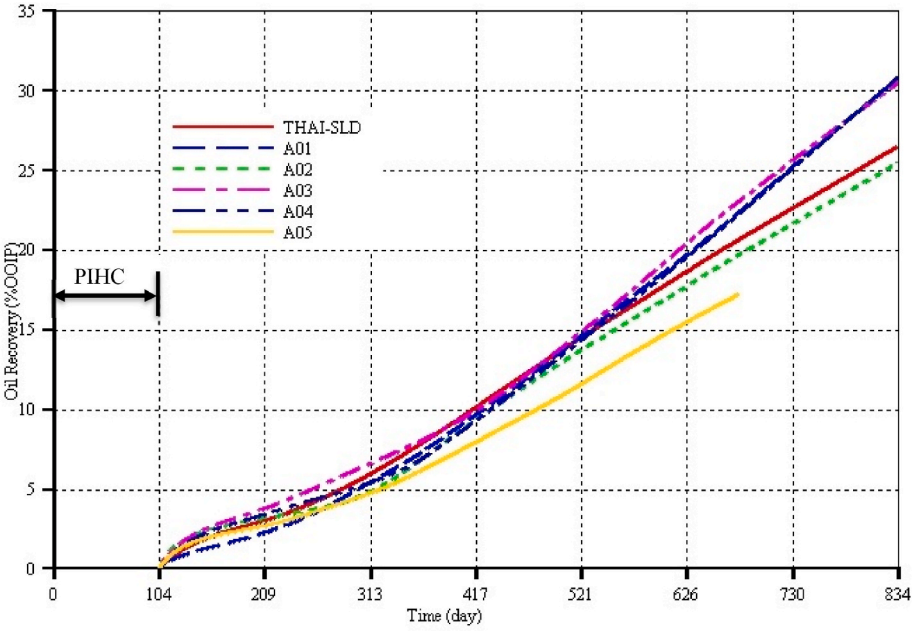

Fig. 11. Combined cumulative oil recoveries due to combustion only as function of time. Note that the THAI-SLD model has a single HP well which is unlike the other models that each has two HP wells.

of air injection. The rate increased slowly before it stabilised to a value of around 50 m^3/day between 500 days and 650 days (Fig. 7). Thereafter, it declined gradually, reaching a value of roughly 40 m^3/day at the end of the two years of combustion period (Fig. 7). The cumulative oil production values from P2A and P2B, at the end of the nearly 28 months of operation, were 16000 & 20000 m^3, respectively. Throughout the combustion period, oil production from P2A accounts for 45% of the cumulative oil produced (Figs. 8 and 9). The cumulative oil recovery due to PIHC and combustion is 37.5% OOIP (Fig. 10). The combined percent oil recovery due to combustion only is 30.5% OOIP (Fig. 11) which is roughly the same as that achieved in model A01 and higher than that realised in model A02 by a margin of 5.0% OOIP. Furthermore, it is higher than the recovery in the base case model by an additional amount of 4.00% OOIP. In terms of combustion front efficiency and stability, since it has reached the toe of the HP wells, it is likely that prolonging the process would result in unsafe and uneconomical operation.

3.1.4. *Model A04: oil production and recovery*

In this model A04, the HP wells have the same orientations and dimensions as those of the previous models (A01, A02, and A03). However, they are no longer in-line and no longer located in the vertical mid-plane, rather, they are located on the adjacent vertical planes at a lateral distance of 22 m on either side of the vertical mid-plane. The HI well has a short horizontal-section length of 30 m and it is perpendicular to the axial direction of the HP wells (i.e. its horizontal section, in a toe-to-heel manner, is along the ***j*** axis). At the end of PIHC, 6.38% OOIP was

recovered from both producers, with producer P2B accounting for 60% of the share of oil produced during the PIHC. This could be due to the proximity of the heel of the horizontal injector (HI) well to the toe of producer P2B. Just like in the case of the previous models A01, A02, and A03, the combined oil production rate declined steadily upon air injection to a lowest value of 15 m^3/day at around 70 days after the start of air injection (Fig. 7). As the combustion heat is distributed within the reservoir, the oil rate picked up and steadied out at around 47 m^3/day between 470 and 630 days from the start of the process. Thereafter, until the end of the two years of combustion, the oil rate eventually became, on average, relatively constant at a value roughly equal to 53 m^3/day (Fig. 7). The cumulative oil production from HP wells P2A and P2B are, respectively, 13630 m^3 and 22300 m^3 at the end of 28 months of operation (Figs. 8 and 9). This means a combined cumulative recovery of 37.24% OOIP (Fig. 10) in which 62% of it is due to production via HP well P2B only. The cumulative oil recovery for the two years of combustion only is 30.88% OOIP (Fig. 11) which is approximately the same as that achieved in models A01 and A03 but larger than that in the base case model by around an additional of 4.38% OOIP.

3.1.5. Model A05: oil production and recovery

This model A05 is very similar to model A02 except that a single vertical injector (VI) well in a direct line drive (DLD) is used in the former, which is in place of the HI well that is used in the latter. At the end of the PIHC, 7.2% OOIP, which is the highest when compared to any of the models, is recovered (Fig. 10) in this model A05. It should be noted that this model A05 was run for 676 days of process time because the simulation became too expensive to continue since the requisite time step was becoming very small. The cumulative oil productions, by the end of the 676 days of operation, are 11,000 m^3 and 12,000 m^3 via the HP wells P2A and P2B, respectively (Figs. 8 and 9). This shows that all the two HP wells are used for oil production which is similar to all the other models except A01 and THAI-SLD models. When compared with all the models at 676 days, it can be seen that this well pattern has the lowest combined cumulative oil recovery of 24.5% OOIP (Fig. 10). Furthermore, based on the combined cumulative oil recovery due to combustion only, this model has the lowest value of 17.3% OOIP at the 676 days of operation as can be seen in Fig. 11. This value is less than that of model A02 and the base case model by values of 2.6% OOIP and 3.70% OOIP respectively at the same time of 676 days of operation.

3.2. Quantity of oxygen produced and its utilisation

Starting with the base case model (i.e. THAI-SLD), it can be seen that oxygen production began at 234 days (i.e. 130 days after the initiation of air injection and combustion) (Fig. 12). Thereafter, there is gradual increase in the amount of the produced oxygen until 540 days, at which point, the slope of the cumulative oxygen production curve increased relatively abruptly which is an indication of an increase in the production rate. Beyond 624 days, until the end of the two years of combustion, the increase in the oxygen production is slow. Overall, the oxygen utilisation efficiency in the THAI-SLD model is 99.6%.

For model A01, oxygen production began at around 442 days (i.e. 338 days after the commencement of combustion). However, the production rate is still very low, to the extent that the slope of the cumulative oxygen production is negligibly small until around 624 days, when it became pronounced (Fig. 12). Cumulatively, the oxygen utilisation efficiency is 99.8% which is higher than in the base case model by an additional of 0.2%. This shows that model A01 performs better than the base case model.

In model A02 significant oxygen production began as early as 234 days after the start of the process (i.e. 130 days after the beginning of air injection). After two years of combustion, the oxygen utilisation has fallen to 97.3%. This is extremely low when compared to that in the base case and A01 models respectively. It also appears that the oxygen utilisation will continue to decrease as the process time is extended into many more years (Fig. 12). This is because the combustion front has already traversed some distance along the toes of the producers as shall be seen in Fig. 14d.

In model A03, the oxygen production began 544 days after the start of the process (i.e. 440 days from beginning of air injection) and it appeared to be due to partial instability of the combustion front. This is because of the, at least, two periods (i.e. between 650 and 728 days, and between 754 and 832 days) in which the oxygen production rates are zero, as reflected by the horizontal sections of the A03 model curve in Fig. 12. A partial instability of the combustion front takes place when there is intermittent production of oxygen due to alternation in the concentration of coke ahead of the combustion front. Cumulatively, at the end of the two years of combustion, the oxygen utilisation is 99.5% which is less than that in the base case model and model A01 by 0.1% and 0.3% respectively. Furthermore, as the combustion front already

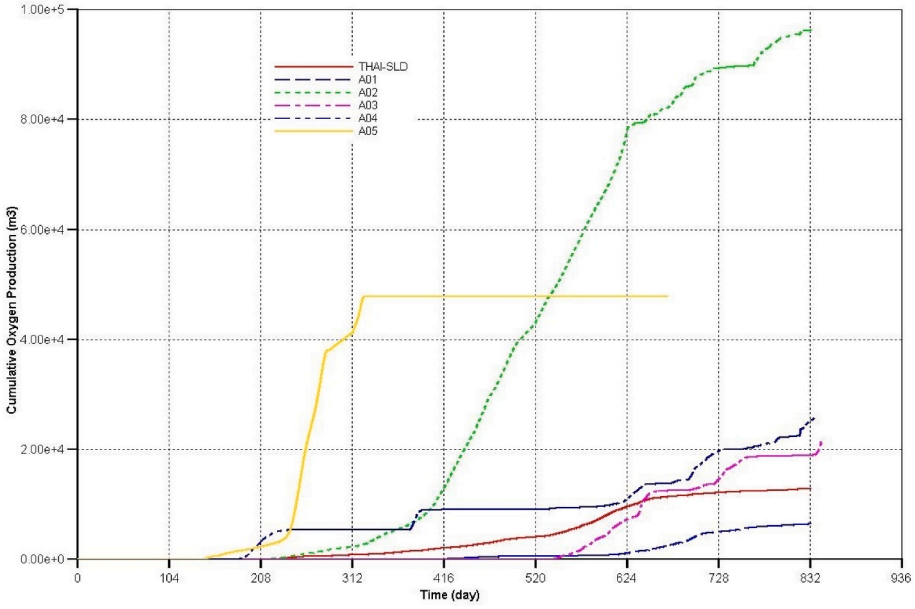

Fig. 12. Combined cumulative oxygen production from the HP well(s) as function of time. Note that the THAI-SLD model has a single HP well which is unlike the other models that each has two HP wells.

reached the toe of the horizontal producers as can be seen in Fig. 14f, the oxygen production is expected to enter a semi-breakthrough period (i.e. between partial instability and breakthrough) in which its production increases with the extension of process operating time. This is because the offset distance between the toe of either of the HP wells and the horizontal section of the HI well is only 7 m which is not very large.

In model A04, oxygen production began at around 180 days from the start of operation (i.e. 76 days after the onset of air injection) (Fig. 12). However, it appeared, for the most part of the combustion period, to be caused by partial instability due to intermittent production as reflected by the horizontal sections of the model A04 curve in Fig. 12. Beyond 624 days of the start of the process (i.e. 520 days after beginning air injection), the oxygen production increased and the trend continued up to the end of the two years of combustion (Fig. 12). The combustion is likely to take a while before it enters a semi-breakthrough phase when the process operation time is prolonged. This is because, no part of the horizontal section of the HI well lies directly on the same vertical plane with any section of either of the two HP wells. Overall, the oxygen utilisation in this model is 99.3% which is lower than those of models THAI-SLD, A01, and A03 but significantly higher than that of model A02.

In model A05, oxygen production began as early as 150 days after the start of the process (i.e. 46 days after the start of air injection). This is the earliest when compared to any of the other models (Fig. 12), and it becomes significant at 234 days. It is evident that locating the VI well on the same vertical mid-plane as, and at 7 m offset distance from, the toe of the HP wells meant that the combustion front will not take long before it can reach the producers, and, thus, cause a significant quantity of oxygen to be produced. However, like in models A03 and A04 respectively, the oxygen production in this model is due to partial instability of the combustion front as reflected by the period of no oxygen production (i.e. the horizontal section of the A05 curve in Fig. 12) from 320 days to 676 days. This is not anomalous for the following two reasons: (1) the zone along the HP wells on the vertical mid-plane has the highest temperatures (Fig. 14i) when compared to the other models. This implied that, in this model, the air-cooling effect around the HP wells is not significant yet., and (2) the injected air gets into the reservoir via a single injector which has one perforation in its shoe. This meant that the air is entering at a higher velocity than in any other model. For these two reasons, the rate of the coke combustion reaction in model A05 in the HP wells region is higher and this, in turn, led to a higher rate of oxygen consumption. Therefore, these occurrences are what limited the oxygen production in model A05. Once the air-cooling effect around the HP wells becomes significant, a large volume of oxygen is going to be produced. Had it been it was possible to run the simulation until 834 days, like in the other models, it is expected that the cumulative oxygen production curve would increase, though not to the same extent as in model A02. Cumulatively, the oxygen utilisation in model A05 is 98.4% which is substantially smaller than that of the base case, A01, A03, and A04 models respectively but larger than that in model A02.

3.3. Comparison of performance based on the quantitative selection criteria

Table 3 summarises and compares the performance of each model in terms of the combined cumulative oil recovery during PIHC and combustion respectively, and in terms of the combined oxygen utilisation efficiency and onset of oxygen production respectively. Table 3 shows that at the end of the PIHC, model A05 has the highest cumulative oil recovery. Over the same time period, it is followed by models A03, A02, and A04 in that order. The worst performing configuration in terms of cumulative oil recovery at the end of the PIHC is that of model A01, and it is followed by the base case model (i.e. THAI-SLD model). In other words, all the new configurations, except that of model A01, perform better than the base case model in term of the combined cumulative oil recovery at the end of the PIHC. Furthermore, from Table 3, it can be seen that at the end of the two years of combustion only, the combined cumulative oil recoveries in models A01, A03, and A04 are higher than that of the conventional THAI-SLD process by additional amounts of 4.28%, 4.00%, and 4.38% OOIP respectively. These are despite the fact that the THAI process has staggered line drive configuration, and a study by Rabiu Ado (2017) has shown that it performs far better than that when the wells are in a direct line drive configuration. The combined cumulative oil recoveries of models A02 and A05 are, respectively, generally lower than that of the original THAI-SLD base case model. In terms of oxygen utilisation efficiency, only model A01 performs better than the base case model. Model A03 is quite close to the base case model, as they only differ by a margin of 0.1% O_2 utilisation efficiency.

Table 3
Comparison of performance of all the models.

Model name	Combined oil recovery during PIHC (%OOIP)	Combined oil recovery due to combustion only (%OOIP)	Onset of oxygen production after the start of air injection (days)	Combined oxygen utilisation efficiency (%)
THAI-SLD	5.10	26.50	130	99.6
A01	2.85	30.78	338	99.8
A02	6.81	25.50	130	97.3
A03	6.98	30.50	440	99.5
A04	6.38	30.88	76	99.3
A05	7.20	17.30[a]	46	98.4[b]

[a] This figure is after 572 days from the start of air injection and commencement of combustion. Over the same specific combustion period, this value is lower than those in the other models.

[b] This figure is at 572 days after the start of air injection and initiation of combustion. At this time, the combined oxygen utilisation efficiency of model A05 is lower than that of any of the other models except that of model A02.

The results in Table 3 are rated based on the number of the models (i.e. 6). The model that has the best performance compared to any other model is assigned a score of 6 and that which has performed worst compared to any other model is assigned a score of 1. Each of the selection criterion is assigned a given weight based on its relative importance and the time period over which the set criterion is obtained in. At the end, each score is multiplied with the corresponding weight percent of each of the selection criterion. Thereafter, the product scores are summed together and the model with the highest overall score is considered the best and that with the lowest overall score is considered the worst. Table 4 shows that model A01 has the highest score, and it is followed by model A03, which in turn is followed by model A04. The configurations of these three models perform respectively far better than the configuration of the base case model. Model A05 performs far worst and is closely followed by model A02. The base case model is by far more efficient than these last two models. It should be noted that the score of 6 in terms of the combined oil recovery at the end of PIHC and which is obtained by model A05 does not mean that if the process is to continue to be run by injecting steam, rather than injecting air and initiating combustion, that best performance will continue to be obtained. In fact, it will be the opposite, because, just like it (i.e. model A05) has the earliest oxygen production, it will also have the earliest steam breakthrough, which will lead to inefficient and thus unprofitable operation. It is worth pointing out at this stage that the selection criteria developed in Table 4 are not the only performance indicators that must be used to choose the safest, most efficient, and most stable configuration. The reservoir dynamics must also be considered, and they can be investigated from the oil saturation, temperature, and oxygen distributions profiles. Thence, they are the subject of some of the subsequent sections. However, since 3 of the novel methods, namely models A01, A03, and A04, perform quantitatively far better than the base case model, the latter is not included in the qualitative analyses that will follow. At this point, and as a useful point of information, it is critical to draw the attention of the reader that although we have used the percentage of oxygen utilisation for screening the models, it is important to strongly point out that the oxygen utilisations in all the models are excellent, and

Table 4
Score for each model based on four selection criteria (i.e. 4 performance indicators).

Performance indicator (weight)[a]	Combined oil recovery during PIHC (6%)	Combined oil recovery due to combustion only (44%)	Onset of oxygen production after the start of air injection (20%)	Combined oxygen utilisation efficiency (30%)	Total score
Model name					
THAI-SLD	2	3	4	5	3.74
A01	1	5	5	6	5.06
A02	4	2	4	1	2.22
A03	5	4	6	4	4.46
A04	3	6	2	3	4.12
A05	6	1	1	2	1.60

[a] The weight of each performance indicator is put as a percentage inside a bracket under the name of that indicator.

can be considered almost 100%, for practical purposes.

3.4. Oil saturation profiles

The oil saturation gives clear information about the oil flow dynamics inside the reservoir. Fig. 13 shows the oil saturation profiles along the vertical (left) and the horizontal (right) (or ***i-k*** and ***i-j***) mid-planes of the reservoir respectively, and these are for all the models except the base case whose details can be found in a recently published study by Ado (2021d), and all are at the end of the two years of combustion period (i.e. 834 days of process operation) except those of model A05 which are at the 676 days after the start of the process operation. Additionally, the extent of displacement of oil in the vertical and horizontal mid-planes (or mid-planes ***i-k*** and ***i-j***) respectively are enough to give a qualitative measure of the degree of reservoir volume swept. The vertical mid-plane (or mid-plane ***i-k***) of model A02 is mostly swept and thus produced (Fig. 13c) when compared with those of the other models. This is followed by model A03 (Fig. 13e), then by model A05 even though it was run for only 676 days (Fig. 13i), then by model A01 (Fig. 13a), and finally by model A04 although none of the HP well in model A04 is located on the vertical mid-plane (Fig. 13g). The implication of rapid high areal or volumetric sweep on the vertical mid-plane (or mid-plane ***i-k***), for the models whose HP wells are located there, is that when only a small amount of, or no, oil is left to be cracked for coke (or fuel) deposition, and once the combustion front reaches there, the oxygen, especially if the HI well or VI well(s) is(are) located on that plane, will have a direct path via which it will be channelling into the HP well(s). This will not only lead to a decrease in oil production rate and economic returns, due to a decrease in rate of heat generation, but also could lead to potentially disastrous events such as explosion in the HP well(s), excessive corrosion, etc.

Observing the horizontal mid-planes (or mid-planes ***i-j***) (Fig. 13, right), the middle of the lateral edges on either side of the reservoir in model A01 has been swept and prolonging operation will lead to more oil being produced not only from the axial vertical planes (or the ***i-k*** planes) immediately adjacent to the vertical mid-plane (or mid-plane ***i-k***) but also from the vertical planes (or ***i-k*** planes) at the lateral edges of the reservoir (Fig. 13b). In other words, the oil located on the lateral vertical planes (or ***j-k*** planes) on either side of the oil-drained zone of Fig. 13b will be stably and efficiently produced if the process is operated for an additional period of time. For this model A01, however, it should be noted that the oil-drained zone is not fully symmetrical for the simple reason mentioned earlier in section 3.1.1. Now, contrasting A01 with the model A02 which also has asymmetrical oil-drained zone (Fig. 13d), it can be seen that the oil-drained zone in model A02 is located along the axial vertical mid-plane (or mid-plane ***i-k***) and along its immediate adjacent vertical planes (or ***i-k*** planes) on its either side to the extent that all the oil on those planes at the axial edge on the side of P2A well is produced. In other words, all or a significant quantity of oil that is present on the axial vertical (or ***i-k***) planes at and near the lateral edges of the reservoir is untouched and not produced, and it is likely that extending the operating period will lead to unstable, inefficient, and unsafe operation. In the case of model A03 (Fig. 13f), the oil-drained zone is symmetrical both laterally and axially. The oil-drained zone is about to reach the centre of the axial vertical (or ***i-k***) planes located on either lateral end of the reservoir. Once it is there, oil displacement will be axially due to the no flow boundary condition. Axially, there is preferential displacement of oil in the centre of the reservoir which will lead to the vertical mid-plane (or mid-plane ***i-k***) being swept earlier than any other adjacent axial vertical (or ***i-k***) planes. However, the process operation can be extended for a long period of time before the efficiency, stability, and safety of the model A03 process are compromised. Similar to model A01, in model A04, the mid of the lateral edges of the reservoir has been swept, and extending process operation time will result in more oil being produced from the axial vertical planes (or ***i-k*** planes) located at the lateral edges (Fig. 13h). In this model A04, at and near the axial edges on either side, all or nearly all the oil there, which is substantial in quantity, is untouched, thereby implying that, should the process operation time be extensively prolonged, a substantial quantity of oil will be recovered whilst the process still operates stably, efficiently, and safely. Model A05 has the highest quantity of oil on the horizontal mid-plane (or mid-plane ***i-j***) (Fig. 13j) as compared to any of the other models. This is partly caused by the fact that the process is operated for only 676 days which is unlike in any of the other models. Therefore, it is anticipated that should the process operating time be extended until 834 days, more oil will be displaced and produced. However, the quantity of the oil that will be left on the layer K4 (or ***i-j*** plane 4 when counting from the top) will still be higher than that in any of the other models since, on average, model A05 has the lowest oil production rate during most of its combustion period and hence it has the lowest recovery factor (Fig. 11). On the other hand, the oil that will be left in the axial vertical mid-plane (or mid-plane ***i-k***) will be far lower than that in any of the other models, and therefore, the concentration of coke that is, and will be, deposited on this plane is, and will be, very low. This implies that the combustion front is certainly going to start to propagate inside the HP wells. Therefore, from the aforementioned, as seen before (Fig. 12), and as will be shown in Fig. 14j, where it reveals that the combustion front has propagated along the vertical mid-plane (or mid-plane ***i-k***) onto which the HP wells are located, this process is unstable, inefficient, and unsafe.

Therefore, to summarize, from the perspective of the oil saturation distribution, in terms of both short and long term stability, model A05 is the least stable, which is followed by model A02. On the other hand, model A04 is the most stable, which is then followed by model A01. Model A03 is in the middle of those two extremes. To expand further, at first, it might not be obvious that model A04 is the most stable compared to models A01 and A03, which is because the HP wells of the former are not located on the vertical mid-plane (or mid-plane ***i-k***). However, digging deeper, it can be seen that the oil in the second to the last bottom horizontal layer (i.e. K6 or ***i-j*** plane 6 when counting from the top), as can be seen in Fig. 13g, is mostly not produced and, therefore, it is conclusively evident that directly above the HP wells, which are on the bottom horizontal layer (i.e. layer K7), there is a layer of oil whose saturation most likely ranges from 38 to 100%. Further, oil must first be produced before the combustion will start to propagate along the HP

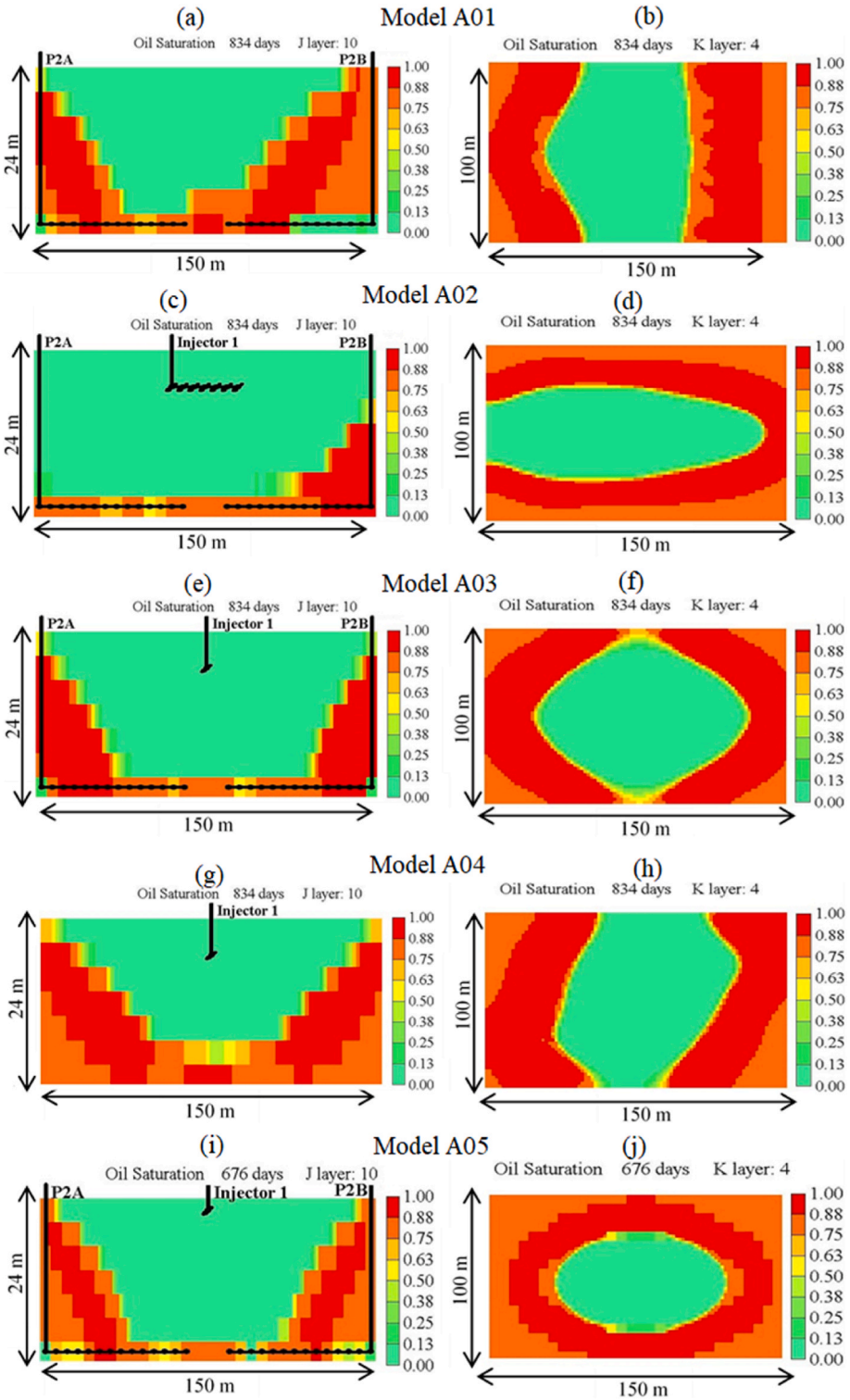

Fig. 13. Oil saturation profiles along the vertical mid-planes (or mid-planes ***i-k***) (left) and on the horizontal mid-planes (or mid-planes ***i-j***) (right) of the 5 reservoir models with novel wells configurations.

wells, even though the HP wells are not located on the axial vertical mid-plane (or mid-plane ***i-k***). The models are arranged in order of decreasing performance as follows: A04 > A01 > A03 > A02 > A05.

3.5. Temperature and oxygen profiles

The temperature and oxygen profiles give the extent of heat-affected area and volume, and the extent of areal and volumetric sweep of the reservoir by the combustion front, respectively. In model A01, the combustion front has not reached the vertical mid-plane (or mid-plane ***i-k***) where the HP wells are located (Fig. 14a and b, and 15a & 15b). Heat transfer from the combustion-swept zone and combustion front resulted in the temperature of that plane increasing to up to 330 °C (Fig. 14a), whilst the maximum concentration of oxygen in that plane is only 2.1 mol% (Fig. 14b). The combustion zone is very well-structured as it propagates in ring forms that are yet to intersect and form a single

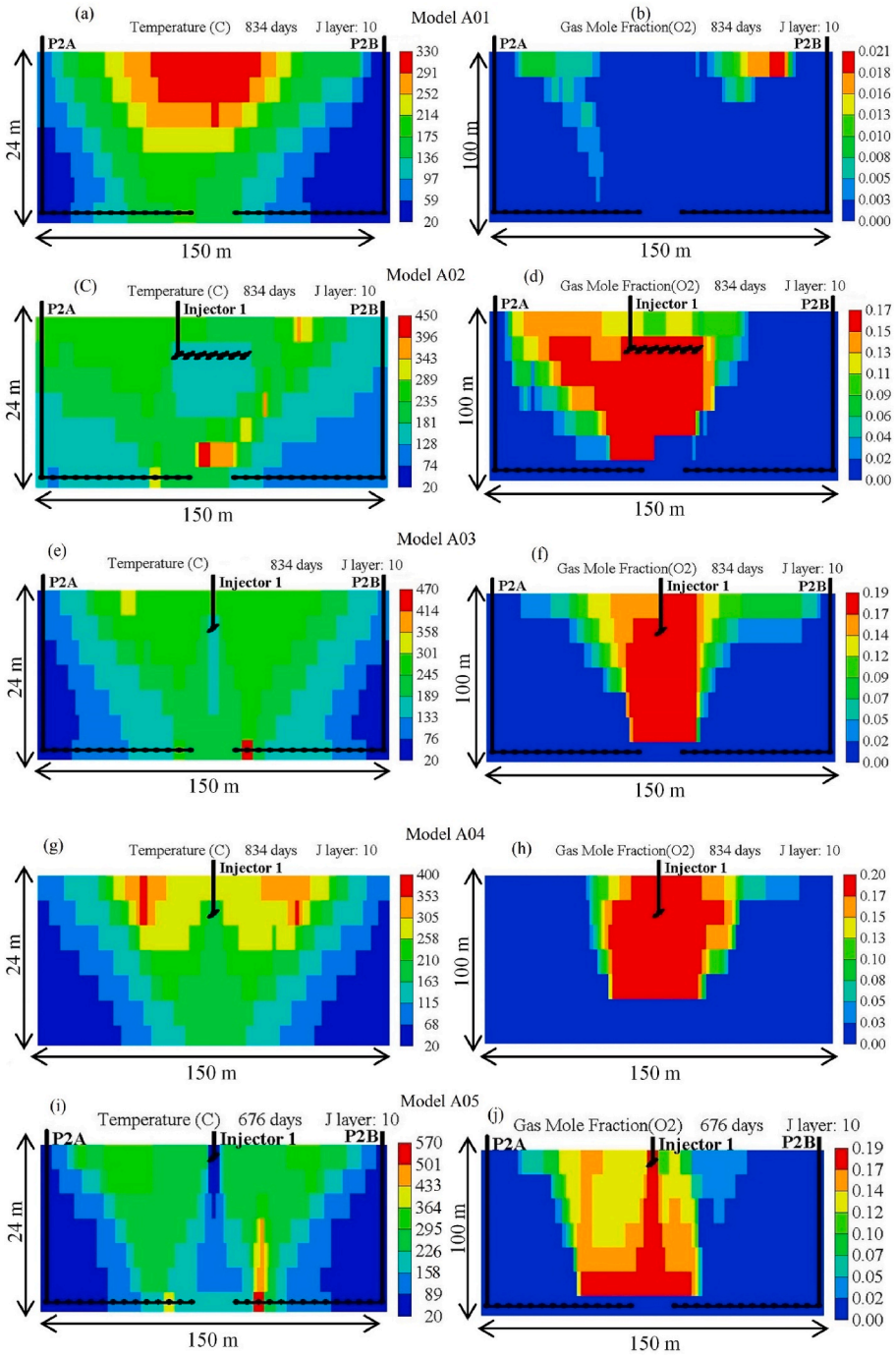

Fig. 14. Temperature distribution (left) and oxygen distribution (right) profiles along the vertical mid-planes (or mid-planes ***i-k***) of the 5 reservoir models with novel wells configurations.

chamber (Fig. 15a & b). Once they intersect, it means the combustion is now propagating on the vertical mid-plane (or mid-plane ***i-k***). However, the process has to be run for a far longer time before they (i.e. the two combustion chambers) overlap each other, and this will lead to unstable, inefficient, and unsafe operation once the combustion front starts to propagate inside the HP wells. In models A02, A03, and A05, the combustion fronts are propagating along the vertical mid-plane (or mid-plane ***i-k***) to the extent that they have reached the horizontal plane K6 (or second to the last ***i-j*** plane when counting from the top) that is just overlying the bottom-most horizontal plane (or bottom-most ***i-j*** plane) onto which the HP wells are located (Fig. 14d, f, & 14j). Among these three models, model A03 is the most stable as the combustion zone swept relatively only a small area around the toes of the HP wells which is unlike model A02 whose combustion zone has swept a relatively large area in the vicinities of the toes of the HP wells. The combustion-swept area around the toes of the HP wells of model A05 is the largest when compared to those of models A02 and A03. The reaching of the toes of the HP wells by the combustion front, and/or its propagating along the HP wells, are/is not the only cause/s of instability and inefficiency in these in-situ-combustion-type processes. In other words, any of these models can become inefficient and unstable due to combustion fronts reaching the toe regions of the HP well and/or propagating along the HP wells, and/or due to oxygen channelling or bypassing the combustion fronts, and/or due to failure of the coke or mobilised oil to provide the

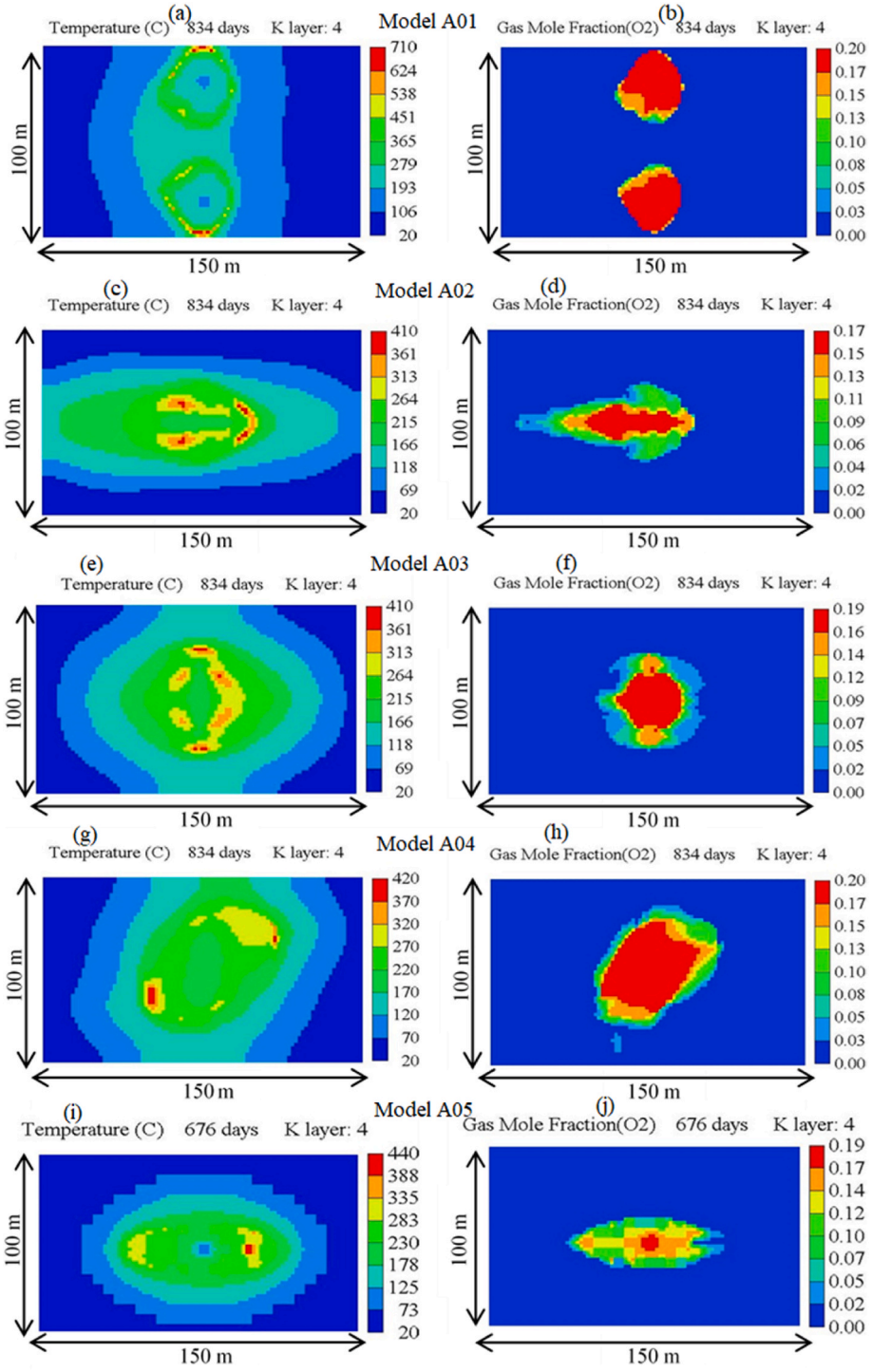

Fig. 15. Temperature distribution (left) and oxygen distribution (right) profiles on the horizontal mid-planes of the reservoirs.

necessary sealing required to prevent oxygen/air breakthrough into the HP well(s). Therefore, since these are the cases, closer examinations of the oxygen profiles are warranted. Thence, observing the zones around the heels and the legs of the HP wells, it can be seen that the combustion fronts of models A02 and A05 are skewed toward the left axial edge of the respective reservoirs (i.e. toward the side of the HP well P2A of each model), and that of model A02 has swept the largest area when compared to that of model A05. Furthermore, the concentrations of oxygen, in the form of mole fractions, are mostly significantly higher in model A02 in those regions when compared to those of model A05 in similar regions (Fig. 14d & j). Consequently, more oxygen will reach the HP well P2A and get produced in model A02 than in model A05. Furthermore, models A02 and A05 have significant air-cooling effects (Fig. 14c & i) that will eventually lead to the dying out of combustion along the vertical mid-plane which will in turn result in air having a direct pathway to the HP wells. The air-cooling effect in model A05 exceeded that in model A02 by far, as the maximum temperature in the vicinities of the VI well of the former is 89 °C (Fig. 14i) while that around the HI well of the latter is 181 °C (Fig. 14c). These findings imply that model A02 is the least stable and least efficient model, and it is followed by model A05. In model A03 (Fig. 14e), the air-cooling effect is relatively less intense compared to in model A02. Therefore, the certain

conclusion that can be drawn from the aforementioned discussion is that model A03 is, by far, more stable, efficient, and safer than model A05, which in turn is much more stable, efficient, and safer than model A02. However, model A03 is less safe, efficient, and stable than model A01. In model A04, just like the observation made from the oil saturation profiles, the combustion front is yet to reach horizontal layer K6 (or 2nd to the last bottom ***i-j*** plane) which directly overlies the bottom-most horizontal layer K7 where the HP wells are located (Fig. 14h). However, this does not mean that the combustion front has not reached the horizontal layer K6 at every location. Furthermore, the HP wells of model A04 are not located on the vertical mid-plane (or mid-plane ***i-k***), and since the area whose oxygen concentration in form of mole fraction ranges from 0.17 to 0.20 is higher than that of model A03, it follows that the fully swept area by the combustion front in model A04 is higher than that in model A03. Additionally, the axial spread of the region with the highest concentration of oxygen (i.e. the distance covered in the ***i*** direction by the region with the highest concentration oxygen) in model A04 is higher than that in model A03. Therefore, the combustion front in model A04 is going to reach the heel and leg regions of the HP wells earlier than that in model A03. These imply that model A04 is less stable and less efficient than model A03. On average, model A04 experiences an insignificant air-cooling effect in the vertical mid-plane (or mid-plane ***i-k***) (Fig. 14g) when compared to models A02, A03, and A05. However, this again will not be a problem since the HP wells of model A04 are not located in the vertical mid-plane (or mid-plane ***i-k***). Since the maximum mole fraction (or partial pressure) of oxygen on the vertical mid-plane (i.e. mid-plane ***i-k***) of model A04 is far larger than that in model A01, it means the former is more prone to oxygen production than the latter, especially if the fact that the concentration of the coke being deposited in model A01 is almost twice that in model A04 is considered.

Fig. 15 shows the temperature and oxygen profiles respectively for each model along the horizontal middle layer of the reservoir. Comparing them shows that the shape of the combustion zone is much more well-structured in model A01 (Fig. 15a & b) than in any other model. Furthermore, in accordance with the earlier findings from oxygen utilisation efficiency, the temperature of the combustion zone in model A01 is higher than that of any of the other models. Additionally, model A01 has a combustion front skewed to the left which is caused by the preferential displacement of oil toward the HP well P2A during the PIHC. However, the skewedness is not as pronounced as that of model A02 in which the combustion front almost reaches the left axial edge of the reservoir (Fig. 15c & d). In this model A02, oxygen has the greatest tendency to reach the HP well P2A and get produced due to bypassing of combustion fronts and/or channelling which are/is manifested by the excessive gas override. Models A03, A04, and A05 (Fig. 15f, h, & 15j) have more-structured combustion fronts than in model A02 which is far less structured than in model A01. Model A05 swept the smallest area, which can be associated with the fact that it is run for only 572 days of combustion and that it has the second lowest oxygen utilisation efficiency, when compared to any other model (Fig. 15, right). For all the other models that are run for 730 days of combustion, the smallest area is swept by the combustion front in A02, which is followed by model A03. In contrast, the largest area is swept by the combustion front in model A01 which is followed by model A04. These findings are very important because the larger the area swept by the combustion front, the greater the heat distribution in the reservoir (Fig. 15, left) and the higher the mobilisation rate, and, hence, production rate of the oil. Moreover, in some cases, higher oxygen utilisation efficiency is a reflection of the higher areal and volumetric sweeps by the combustion front as the otherwise oxygen to be lost is consumed. However, in some other cases, higher areal and volumetric sweeps lead to instability and inefficiency especially if the sweeping takes place rapidly around the HP wells. Therefore, observing Fig. 15f and h, it can be seen that model A04 has higher areal sweep than model A03, and this implies that the combustion front in model A04 will reach the heel and leg regions of the HP wells more than in model A03. It hence follows that, should the process operating times be extended, model A04 will become unstable, inefficient, and unsafe first before model A03.

To summarize, from Figs. 14 and 15, model A01 performs better than any other model, and it is followed by model A03. On the other hand, model A02 performs worse than any other model, and it is followed by model A05. These mean that model A04 is in between these two extremes. The models are arranged in order of decreasing performance as follows: A01 > A03 > A04 > A05 > A02.

3.6. Comparison of performance based on the qualitative selection criteria

Table 5 summarises and compares the performance of each of the novel models in terms of the oil flow dynamics inside the reservoir in the form of oil saturation distribution, and in terms of temperature distribution and combustion front spread in the form of oxygen distribution. The model that performs the best is assigned a value of 5 and that which performs the worst is assigned a mark of 1, and the rest are in between these two extremes. Since the stability and efficiency of the combustion inside the reservoir is far more important, as it is the determining factor for oil production rate and cumulative recovery, the temperature and oxygen profiles are assigned a weight of 60%, while the oil flow dynamics are assigned a weight of 40%. The sum of the product of the criterion score and the corresponding weight of the criterion for each model are then tabulated under the ‘‘Total score’’ column (Table 5).

Table 5 shows that, qualitatively, model A01 has the highest score and hence it has the best performance. It is followed a little distantly by model A04, which in turn is closely followed by model A03. Model A02 performs by far worst and is closely followed by model A05.

3.7. Selection of the best performing novel method

To select the best performing novel method, the quantitative and qualitative scores, being now the selection criteria, are respectively assigned weights of 60% and 40%. The split is assigned this way because the quantitative parameters are much more important and they give, by far, the clearest picture of the performance of any of the processes. In other words, they allow a decision to be made with nearly full confidence. The quantitative scores for each model, which are given in Table 4, and the qualitative score of each model, which are given in Table 5, are then correspondingly multiplied with the weight of each selection criterion. The sum of the products of the criterion score and weight gives the overall score for each model (Table 6).

Table 6 shows that the novel process named model A01 has the overall best performance and it is followed by model A03. Model A05 performs worse than any other model, and it is closely followed by model A02.

4. Conclusions

The key findings from these in-depth studies are summarised as follows:

Table 5
Score for each model based on the two qualitative selection criteria.

Selection criteria (weight)[a]	Stability and efficiency of combustion in form of temperature and oxygen distribution profiles (60%)	Oil flow dynamics in form of oil saturation profiles (40%)	Total score
Model name			
A01	5	4	4.6
A02	1	2	1.4
A03	4	3	3.6
A04	3	5	3.8
A05	2	1	1.6

[a] The weight of each selection criterion is put as a percentage inside a bracket under the name of that criterion.

Table 6
Score for each model based on the quantitative and qualitative selection criteria.

Selection criteria (weight)[a]	Quantitative performance from Table 4 (60%)	Qualitative performance from Table 5 (40%)	Overall score
Model name			
A01	5.06	4.6	4.88
A02	2.22	1.4	1.89
A03	4.46	3.6	4.12
A04	4.12	3.8	3.99
A05	1.60	1.6	1.60

[a] The weight of each selection criterion is put as a percentage inside a bracket under the name of that criterion.

i) New THAI arrangements have been developed and studied by means of simulation for the case of oil formations with extremely low dip (less than 2–3°), namely so-called flat formations.
ii) In the case of flat formations, 5 new arrangements (A01 to A05) were considered with the possibility of further developing the field - initiating new patterns – in opposite directions. Their efficiency was compared with that of the classic THAI-SLD configuration, which, however, can be applied for both flat and high dip formations. Keeping note that the THAI-SLD process has higher oil production rates than when configured in a direct line drive (DLD) configuration, it is found that indeed the oil production rates and cumulative oil recovery can be considerably improved with the stable, efficient, and safe combustion front propagation when the wells are reconfigured compared to that achievable in the conventional THAI process.
iii) Only A01 and A05 arrangements had vertical air injectors and the study confirmed again that in these cases the SLD configuration is superior to the DLD configuration (comparison of A01 and A05 models). As the arrangements A02 to A04 had horizontal injectors, the results from their simulation may be used in the future, when technological advances will justify that use.
iv) Based on rigorous selection criteria it was found that arrangements A01 and A03 had the best performance, which was better than the base case of the classic THAI-SLD configuration. However, it should be noted that, since arrangement A03 has a horizontal injector, it will cost more to drill and operate and, therefore, proper economic evaluation should follow before considering it further
v) For oil formations with extremely low dip, future developmental work should concentrate on arrangement A01 since it has the highest oxygen utilisation, which is 99.8%, and higher cumulative oil recovery due to combustion only of 4.28% OOIP more than that from the conventional THAI-SLD process. However, the choice between the A01 arrangement and classic THAI-SLD should be based on economic calculations for the specific case, as the A01 arrangement involves drilling an extra horizontal production (HP) well (i.e. A01 configuration has two HP wells, with each HP well having half the length of the HP well of the THAI-SLD) for the draining of the same volume of reservoir.

CRediT authorship contribution statement

Muhammad Rabiu Ado: Writing – review & editing, Writing – original draft, Visualization, Validation, Software, Methodology, Investigation, Funding acquisition, Formal analysis, Data curation, Conceptualization. **Malcolm Greaves:** Writing – review & editing, Visualization, Validation, Supervision, Software, Resources. **Sean P. Rigby:** Writing – review & editing, Supervision, Software, Resources, Project administration, Funding acquisition.

Declaration of competing interest

The authors declare that they have no known competing financial interests or personal relationships that could have appeared to influence the work reported in this paper.

Data availability

Data will be made available on request.

Acknowledgements

The authors are grateful to the Computer Modelling Group (CMG) for supplying comprehensive reservoir simulator, the STARS.

References

Ado, M.R., 2022a. Comparisons of predictive ability of THAI in situ combustion process models with pre-defined fuel against that having fuel deposited based on Arrhenius kinetics parameters. J. Pet. Sci. Eng. 208, 109716 https://doi.org/10.1016/j.petrol.2021.109716.
Ado, M.R., 2022b. Electrically-enhanced THAI in situ combustion technology for upgrading and production of heavy oil. J. Pet. Explor. Prod. Technol. https://doi.org/10.1007/s13202-022-01530-0.
Ado, M.R., 2021a. Use of two vertical injectors in place of a horizontal injector to improve the efficiency and stability of THAI in situ combustion process for producing heavy oils. J. Pet. Explor. Prod. Technol. https://doi.org/10.1007/s13202-021-01345-5.
Ado, M.R., 2021b. Detailed investigations of the influence of catalyst packing porosity on the performance of THAI-CAPRI process for in situ catalytic upgrading of heavy oil and bitumen. J. Pet. Explor. Prod. Technol. 1–15. https://doi.org/10.1007/s13202-021-01345-5.
Ado, M.R., 2021c. Improving oil recovery rates in THAI in situ combustion process using pure oxygen. Upstream Oil Gas Technol., 100032 https://doi.org/10.1016/j.upstre.2021.100032.
Ado, M.R., 2021d. Improving heavy oil production rates in THAI process using wells configured in a staggered line drive (SLD) instead of in a direct line drive (DLD) configuration: detailed simulation investigations. J. Pet. Explor. Prod. Technol. https://doi.org/10.1007/s13202-021-01269-0.
Ado, M.R., 2021e. Understanding the mobilised oil drainage dynamics inside laboratory-scale and field-scale reservoirs for more accurate THAI process design and operation procedures. J. Pet. Explor. Prod. Technol. https://doi.org/10.1007/s13202-021-01285-0.
Ado, M.R., 2020a. Effect of reservoir pay thickness on the performance of the THAI heavy oil and bitumen upgrading and production process. J. Pet. Explor. Prod. Technol. 10 https://doi.org/10.1007/s13202-020-00840-5.
Ado, M.R., 2020b. A detailed approach to up-scaling of the Toe-to-Heel Air Injection (THAI) In-Situ Combustion enhanced heavy oil recovery process. J. Pet. Sci. Eng. 187 https://doi.org/10.1016/j.petrol.2019.106740.
Ado, M.R., 2020c. Predictive capability of field scale kinetics for simulating toe-to-heel air injection heavy oil and bitumen upgrading and production technology. J. Pet. Sci. Eng. 187 https://doi.org/10.1016/j.petrol.2019.106843.
Ado, M.R., 2020d. Simulation study on the effect of reservoir bottom water on the performance of the THAI in-situ combustion technology for heavy oil/tar sand upgrading and recovery. SN Appl. Sci. 2 https://doi.org/10.1007/s42452-019-1833-1.
Ado, M.R., 2020e. Impacts of Kinetics scheme used to simulate toe-to-heel air injection (THAI) in situ combustion method for heavy oil upgrading and production. ACS Omega 5. https://doi.org/10.1021/acsomega.9b03661.
Ado, M.R., Greaves, M., Rigby, S.P., 2021a. Effect of operating pressure on the performance of THAI-CAPRI in situ combustion and in situ catalytic process for simultaneous thermal and catalytic upgrading of heavy oils and bitumen. Pet. Res. https://doi.org/10.1016/j.ptlrs.2021.09.010.
Ado, M.R., Greaves, M., Rigby, S.P., 2021b. Simulation of catalytic upgrading in CAPRI, an add-on process to novel in-situ combustion. THAI. Pet. Res. https://doi.org/10.1016/j.ptlrs.2021.10.002.
Ado, M.R., Greaves, M., Rigby, S.P., 2019. Numerical simulation of the impact of geological heterogeneity on performance and safety of THAI heavy oil production process. J. Pet. Sci. Eng. 173 https://doi.org/10.1016/j.petrol.2018.10.087.
Almehaideb, R.A., Ashour, I., El-Fattah, K.A., 2003. Improved K-value correlation for UAE crude oil components at high pressures using PVT laboratory data. Fuel 82, 1057–1065.
Fatemi, S.M., Ghotbi, C., Kharrat, R., 2009. Effect of wells arrangement on the performance of toe-to-heel air injection. Brazilian J. Pet. Gas 3.
Greaves, M., Al-Shamali, O., 1996. In situ combustion isc process using horizontal wells. J. Can. Pet. Technol. 35 https://doi.org/10.2118/96-04-05.
Greaves, M., Dong, L., Rigby, S., 2012a. Validation of Toe-to-Heel air-injection bitumen recovery using 3D combustion-cell results. SPE Reserv. Eval. Eng. 15, 72–85.
Greaves, M., Dong, L.L., rigby, sean, 2012b. Determination of limits to production in THAI. SPE Heavy Oil Conf. Canada. https://doi.org/10.2118/157817-MS.

Greaves, M., Dong, L.L., Rigby, S.P., 2012c. Simulation study of the toe-to-heel air injection three-dimensional combustion cell experiment and effects in the mobile oil zone. Energy Fuels 26, 1656–1669.
Greaves, M., Tuwil, A.A., Bagci, A.S., 1993. Horizontal producer wells in in situ combustion (ISC) processes. J. Can. Pet. Technol. 32 https://doi.org/10.2118/93-04-04.
Greaves, M., Xia, T.X., Turta, A.T., 2008. Stability of Thai (TM) process - theoretical and experimental observations. J. Can. Pet. Technol. 47, 65–73.
Petrobank, 2014. Petrobank announces Q1 2014 financial and operating results [WWW Document]. URL. http://www.petrobank.com/news. (Accessed 20 May 2014).
Petrobank, 2013. Petrobank reports Q2 2013 financial results and operational update [WWW Document]. URL. http://www.petrobank.com/news. (Accessed 20 May 2014).
Petrobank, 2009. IETP 01-019 Whitesands experimental project – final/annual (2009) report [WWW Document]. URL. https://open.alberta.ca/dataset/06f18b06-8556-45ee-a654-3ff50f25f4f5/resource/8c557fe6-b2a5-44cb-b58d-a27188a67731/download/ietp-approval-01_019-final-and-2009-report.pdf. (Accessed 24 February 2021).
Petrobank, 2008. IETP 01-019 Whitesands experimental project - 2008 annual report [WWW Document]. URL. https://open.alberta.ca/dataset/06f18b06-8556-45ee-a654-3ff50f25f4f5/resource/49c917de-7190-45a1-b92e-334b72a9aa67/download/01-019-ietp-report-with-title-page.pdf. (Accessed 24 February 2021).
Petrobank, 2007. IETP 01-019 Whitesands experimental project - 2007 annual report [WWW Document]. URL. https://open.alberta.ca/dataset/06f18b06-8556-45ee-a654-3ff50f25f4f5/resource/4a1bc69b-6d92-4583-a503-52d36ccaeba9/download/ietp-no.-01-019-whitesands-pilot-economics-2007-annual-report.pdf. (Accessed 24 February 2021).
Rabiu Ado, M., 2017. Numerical simulation of heavy oil and bitumen recovery and upgrading techniques [WWW Document]. URL. http://eprints.nottingham.ac.uk/41502/. (Accessed 20 May 2019).
Rabiu Ado, M., Greaves, M., Rigby, S.P., 2018. Effect of pre-ignition heating cycle method, air injection flux, and reservoir viscosity on the Thai heavy oil recovery process. J. Pet. Sci. Eng. 166 https://doi.org/10.1016/j.petrol.2018.03.033.
Rabiu Ado, M., Greaves, M., Rigby, S.P., 2017. Dynamic simulation of the toe-to-heel air injection heavy oil recovery process. Energy Fuel. 31 https://doi.org/10.1021/acs.energyfuels.6b02559.
Touchstone, 2016. Touchstone announces Kerrobert saskatchewan disposition [WWW Document]. URL. http://www.touchstoneexploration.com/files/6149.January20,2016-KerrobertDisposition-FINAL.pdf. (Accessed 9 May 2016).
Touchstone, 2015. Touchstone announces 2015 third quarter results and elimination of net debt; updates trinidad acquisition [WWW Document]. URL. http://www.touchstoneexploration.com/files/6136. (Accessed 9 May 2016). November 13 2015 - Q3 2015 Results - FINAL - Formatted (002).pdf.
Turta, A., 2018. Toe-to-heel air injection (Thai) process [WWW Document]. URL. https://www.insitucombustion.ca/Advanced_THAI_Brochure.pdf. (Accessed 24 February 2021).
Turta, A., Kapadia, P., Gadelle, C., 2020. Thai process: determination of the quality of burning from gas composition taking into account the coke gasification and water-gas shift reactions. J. Pet. Sci. Eng. 187, 106638 https://doi.org/10.1016/j.petrol.2019.106638.
Turta, A., Singhal, A., 2004. Overview of short-distance oil displacement processes. J. Can. Pet. Technol. 43.
Wei, W., Rezazadeh, A., Wang, J., Gates, I.D., 2020a. An analysis of toe-to-heel air injection for heavy oil production using machine learning. J. Pet. Sci. Eng. 108109 https://doi.org/10.1016/j.petrol.2020.108109.
Wei, W., Wang, J., Afshordi, S., Gates, I.D., 2020b. Detailed analysis of Toe-to-Heel Air Injection for heavy oil production. J. Pet. Sci. Eng. 186, 106704 https://doi.org/10.1016/j.petrol.2019.106704.
Xia, T., Greaves, M., Turta, A., 2005. Main mechanism for stability of Thai-Toe-to-Heel air injection. J. Can. Pet. Technol. 44.
Xia, T.X., Greaves, M., 2002. Upgrading Athabasca tar sand using toe-to-heel air injection. J. Can. Pet. Technol. 41, 7. https://doi.org/10.2118/02-08-02.
Xia, T.X., Greaves, M., Turta, A.T., 2002. Injection well - producer well combinations in Thai “toe-to-heel air injection”. https://doi.org/10.2118/75137-MS.
Zhao, R., Yang, J., Zhao, C., Heng, M., Wang, J., 2021. Investigation on coke zone evolution behavior during a Thai process. J. Pet. Sci. Eng. 196, 107667 https://doi.org/10.1016/j.petrol.2020.107667.
Zhao, R., Yu, S., Yang, J., Heng, M., Zhang, C., Wu, Y., Zhang, J., Yue, X., 2018. Optimization of well spacing to achieve a stable combustion during the Thai process. Energy 151, 467–477. https://doi.org/10.1016/j.energy.2018.03.044.